REPUBLIC OF TÜRKİYE
KIRŞEHİR AHİ EVRAN UNIVERSITY
INSTITUTE OF NATURAL AND APPLIED
SCIENCES
DEPARTMENT OF MECHANICAL
ENGINEERING

INVESTIGATION OF THE EFFECT OF NANOFLUID FLOW ON HEAT TRANSFER IN DOUBLE PIPE HEAT EXCHANGERS

MOHAMMED FLAYYIH HASAN

MSc THESIS

KIRŞEHİR

2023

REPUBLIC OF TÜRKİYE
KIRŞEHİR AHİ EVRAN UNIVERSITY
INSTITUTE OF NATURAL AND APPLIED
SCIENCES
DEPARTMENT OF MECHANICAL
ENGINEERING

INVESTIGATION OF THE EFFECT OF NANOFLUID FLOW ON HEAT TRANSFER IN DOUBLE PIPE HEAT EXCHANGERS

MOHAMMED FLAYYIH HASAN

MSc THESIS

SUPERVISOR
Asst. Prof. Dr. Merdin DANIŞMAZ
II. SUPERVISOR
Dr. Bassim Mohammed Majel AL-KATIB

KIRŞEHİR

2023

LIST OF CONTENTS

ACKNOWLEDGEMENTS

GENİŞLETİLMİŞ ÖZET

YÜKSEK LİSANS TEZİ

ÇİFT BORULU EŞANJÖRLERDE NANOAKIŞKAN AKIŞININ ISI TRANSFERİNE ETKİSİNİN İNCELENMESİ

MOHAMMED FLAYYİH HASAN

KIRŞEHİR AHİ EVRAN ÜNİVERSİTESİ
FEN BİLİMLER ENSTİTÜSÜ
MAKİNE MÜHENDİSLİĞİ ANABİLİM DALI

Günümüzde termal sistemler en kritik teknik altyapıların başında gelmektedir. Bu tür sistemlerde termal performansı en üst düzeye çıkarmak için araştırmacılar, ısı aktarımını artırmaya yönelik çeşitli yöntemler araştırdı ve geliştirdi. Geleneksel ısı eşanjörlerinin ısı transfer hızları çeşitli yüzey geliştirme teknikleri kullanılarak iyileştirilebilir. Isı transferindeki bu artıştan geliştirilmiş yüzey koşulları sorumludur. Sınır tabakası bu koşullar altında oluşamaz; türbülans seviyesi yükselir, ısı transfer alanı artar ve ikincil akışlar oluşur.

Isı eşanjörleri endüstrilerde ısı çıkarma ve geri kazanım sistemlerinde temel üniteler olarak yaygın şekilde kullanılmaktadır. Yüksek performanslı ısı transfer sistemi birçok endüstriyel uygulamada büyük önem taşımaktadır. Çeşitli güçlendirme teknikleri, ısı eşanjörlerin performansını önemli ölçüde artırabilir. Mevcut çalışma, düz boruya kıyasla daha yüksek bir ısı transfer hızına yol açan ısıtma dağılımını iyileştirmek için çift borulu bir ısı eşanjörde dış iç boruya takılan uzatılmış yüzeylerin kullanıldığını rapor etmektedir. Çalışma akışkanı olarak alümina nanoakışkanın kullanıldığı çift borulu bir ısı eşanjörde ısı transfer katsayısı, duvar sıcaklığı ve termal iyileştirme faktörü özellikleri (Nu) sayısal olarak incelenmiştir. Testler hem laminer hem de türbülanslı akış Reynolds sayısı aralıkları için gerçekleştirilir. Düz boru ve düz uzatılmış yüzeye ilişkin sayısal veriler, literatürde mevcut olan standart verilerle doğrulanmıştır.

Bu çalışmada, çift borulu bir ısı eşanjörü karşı akışında hacimce $\varphi = 1, 3, 5\%$ konsantrasyonlarında damıtılmış su ve metal oksit nanoakışkan tipi Al_2O_3'ün akışı ve ısı transfer özelliklerinin iyileştirilmesi incelenmiştir. Test bölümü çift borulu bir ısı eşanjördir. 150 cm uzunluğunda eşmerkezli borulardan yapılmıştır. İç boru olarak dış çapı (22.12 mm) olan bir bakır boru, dış boru olarak ise dış çapı (54.12 mm) olan bir bakır boru seçilmiştir. Sıcak akışkan iç boruda akarken soğutma akışkanı halka içinde akar. Sıcak akışkanın kullanılan giriş sıcaklığı (25°C) olup, Reynolds sayıları 250 ila 2500

arasında değişirken, soğuk suyun akışı, halka boyunca 0.03 ila 0,07 kg/sn arasında değişen kütle akış hızlarına sahiptir.

Çift borulu ısı eşanjörü ANSYS'te Fluent kullanılarak simüle edilmiştir. Türbülansın etkisini göstermek için iki taşıma denklemi (k-ε) modelinin çözümünü içeren bir model kullanılmış ve üç boyutlu geometri oluşturulmuştur. ANSYS versiyonu (20), sabit giriş sıcaklığında su veya nanoakışkan durumu için ısı eşanjörüni simüle etti.

Sonuçlar, sudan nanoakışkana doğru hareket ettikçe akışkanın sıcaklığının arttığını göstermektedir. İç boru boyunca ortalama sıcaklık genel olarak akış hızının artmasıyla sabit kalır. Ayrıca akışkan özelliklerindeki değişiklik Nusselt sayısının değerlerini de arttırır. Nanoakışkan, Prandtl sayısının yüksek olması nedeniyle diğer çalışma akışkanları arasında hacim konsantrasyonu (%5) ve akış hızında (0.07 kg/s) en yüksek Nusselt sayısına sahiptir. Boyuna kanatçıkların ve nanoakışkanın varlığı, tek başına kanatçıkların varlığına göre daha önemli bir Nusselt sayısına sahiptir. Nanoakışkan için Nusselt sayısı artan konsantrasyonla birlikte artar ($_\varphi$= 1, 3 ve %5). Konsantrasyon arttıkça Nusselt sayısı 20'ye yükselir ($_\varphi$= %5, Re=2500). Nusselt sayısı ile Reynolds sayısı arasındaki korelasyonlar, kullanılan her çalışma akışkanı için güç yöntemi kullanılarak yapılır.

Mevcut ısı eşanjörde iç borunun dış yüzeyine kanatçıklar eklendiğinde ısı iletimindeki iyileşme görülmektedir. Bu gelişme, düz boruya göre sırasıyla (2.3 ila 3.1) ve (1.6 ila 2) katı olan ısı yayılımı ve soğuk su ısı transfer katsayısı değerlerinde görülmektedir. Soğuk su tarafındaki sıcaklık farkı, sıcak suyun Reynolds sayısıyla doğrudan ilişkilidir ve soğuk suyun kütlesel debisi arttıkça %57'lik bir azalma yaşanır. Ayrıca elde edilen sayısal sonuçların açık literatür sonuçlarıyla karşılaştırılmasını içeren karşılaştırmalar da iyi bir uyum göstermektedir.

Anahtar Kelimeler: Akışkan akışı, HAD, Isı değiştirici, Nanoakışkan

ABSTRACT

MSc. THESIS

INVESTIGATION OF THE EFFECT OF NANO FLUID FLOW ON HEAT TRANSFER IN DOUBLE PIPE HEAT EXCHANGERS

MOHAMMED FLAYYIH HASAN

KIRŞEHİR AHİ EVRAN UNIVERSITY
INSTITUTE OF NATURAL AND APPLIED SCIENCES
DEPARTMENT OF MECHANICAL ENGINEERING

Supervisor: **Asst. Prof. Dr. Merdin DANIŞMAZ**
                     Yıl: 2023, Pages: 77
Juries: **Asst. Prof. Merdin DANIŞMAZ**
                     Prof. Dr. Ali Osman KURBAN
                     Prof. Dr. Levent URTEKİN
                     Asst. Prof. Nabeel Sameer MAHMOUD
                     Dr. Bassim Mohammed Majel AL-KATIB
Co-Supervisor   **Dr. Bassim Mohammed Majel AL-KATIB**

These days, thermal systems are among the most essential technical infrastructures. In order to maximize thermal performance in such systems, researchers have explored and developed several methods for enhancing heat transport. Traditional heat exchangers may have their heat transfer rate improved by using several surface enhancement techniques. The enhanced surface conditions are responsible for this increase in heat transfer. The boundary layer cannot form under these conditions. The turbulence level rises, the heat transfer area increases, and secondary flows are generated.

Heat exchangers are widely used as essential units in industries' heat-extracting and recovering systems. High-performance heat transfer system is of great importance in many industrial applications. The performance of heat exchangers can be substantially improved by several augmentation techniques. The present work reported using extended surfaces fitted on the outer internal tube in a double pipe heat exchanger to improve the heating dissipation, leading to a higher heat transfer rate than the plain tube. Heat transfer coefficient, wall temperature and thermal enhancement factor characteristics (Nu) in a double pipe heat exchanger using alumina nanofluid as working fluid are investigated numerically. Tests are performed for both laminar and turbulent flow Reynolds number ranges. The numerical data for a plain tube and plain-extended surface are validated with the standard data available in the literature.

In the present work, the flow and the enhancement of heat transfer characteristics of distilled water and metal oxide nanofluid type Al_2O_3 at concentrations of $\varphi = 1, 3, 5\%$ by volume in a double pipe heat exchanger counter flow have been studied. The test section is a double-pipe heat exchanger. It is constructed from concentric tubes with 150 cm in length. A copper tube with an outer diameter of (22.12mm) was chosen as the inner tube and a copper tube with an outer diameter of (54.12mm). The hot fluid flows in the inner tube while the cooling fluid flows in the annulus. The used inlet temperature of hot fluid is (25°C) with Reynolds numbers ranging from 250 to 2500, while cold water flows with mass flow rates ranging from 0.03 to 0.07 kg/sec through annuli.

The double-pipe heat exchanger is simulated using Fluent under ANSYS. To demonstrate the effect of the turbulence, a model that involves the solution of two transport equations (k-ε) model is used, and three-dimensional geometry is generated. ANSYS version (20) simulates the heat exchanger for the case of water or nanofluid at constant inlet temperature.

The results show that the temperature of fluid increases as it moves from the water to the nanofluid. At the same time, the average temperature along the inner pipe remains constant with the increase in flow rate. Also, the change in fluid properties increases the values of the Nusselt number. The nanofluid has the highest Nusselt number at volume concentration (5%) and flow rate (0.07 kg/s) among the other working fluids due to the high Prandtl number. The presence of longitudinal fins and nanofluid has a Nusselt number more significant than that for the presence of fins alone.

For nanofluid, the Nusselt number increases with increasing concentration ($\varphi=1$, 3 and 5%). As the concentration increases, the Nusselt number increases to (20) at ($\varphi=5$%, Re=2500). Correlations between the Nusselt number and Reynolds number are made using the power method for each of the working fluids used.

The improvement in heat transmission is seen when fins are added to the outer surface of the inner tube in the current heat exchanger. This improvement is seen in the heat dissipation and cold water heat transfer coefficient values (2.3 to 3.1) and (1.6 to 2) times that of a smooth tube, respectively. The temperature difference on the cold water side directly correlates with the Reynolds number of the hot water and experiences a reduction of 57% as the mass flow rate of the cold water increases. Also, comparisons, which include comparing the obtained numerical results with open literature results, show a good agreement.

Keywords: Fluid flow, CFD, Heat exchanger, Nano fluid

LIST OF TABLES

LIST OF FIGURES

LIST OF SYMBOLS AND ABBREVIATIONS

Icons		Described
A_c	:	Tube cross-sectional area
A_s	:	Tube surface area
a	:	Annular
avg	:	Average
bf	:	Base fluid
C_p	:	Specific heat
c	:	Cold
D	:	Diameter of outer tube
D_h	:	Hydraulic diameter
E	:	Turbulent kinetic energy dissipation
f	:	Friction factor
H	:	Heat transfer coefficient
h	:	Hot
i	:	Inner
in	:	Inlet
K	:	Turbulent kinetic energy generation
k_f	:	Fluid thermal conductivity
L	:	Length
M	:	Mass
m	:	Mean
$\dot{m}$	:	Mass flow rate
Nu	:	Average Nusselt number
nf	:	Nano fluid
o	:	Outer
p	:	Particle
p	:	Fluid density
p_r	:	Prandtl number

Q	**:**	Heat transfer rate
Re	**:**	Reynolds number
ref	**:**	Reference value
T	**:**	Temperature
U	**:**	Overall heat transfer coefficient
u	**:**	Velocity vector
v	**:**	Kinematics viscosity
w	**:**	Wall
μ	**:**	Dynamic viscosity
Φ	**:**	Heat dissipation term
ΔP	**:**	Pressure drop
η	**:**	Thermal enhancement factor
φ	**:**	Volume concentration percentage

Abbreviations		**Described**
BPN	**:**	Back-Propagation Neural Networks
CFD	**:**	Computational fluid dynamics
GPS	**:**	Global Positioning System
LMTD	**:**	Logarithmic mean temperature difference
RNG	**:**	Renormalization group
SANSS	**:**	Massachusetts Institute of Technology
SIMPLE	**:**	Submerged arc nanoparticle synthesis s

1. INTRODUCTION

These days, thermal systems are among the most important technical infrastructures. In order to maximize thermal performance in such systems, researchers have explored and developed a number of methods for enhancing heat transport. Traditional heat exchangers may have their heat transfer rate improved by the use of several surface enhancement techniques. The enhanced surface conditions are responsible for this increase in heat transfer. The boundary layer cannot form under these conditions, the turbulence level rises, the heat transfer area increases, and secondary flows are generated.

1.1. Modes of Heat Transfer

Within the field of thermodynamics, heat transfer refers to the process by which thermal energy is transferred from a body at a higher temperature to a body at a lower temperature. The phenomenon of thermal energy transmission, commonly referred to as heat transfer, occurs when an object or fluid is at a dissimilar temperature compared to its surrounding environment or another entity. The process of heat exchange continues until the organism and its surrounding environment reach thermal equilibrium. In accordance with the second rule of thermodynamics, it is postulated that in the presence of a temperature disparity between adjacent objects, the cessation of heat transfer is unattainable, as it may solely be impeded. The phenomenon of energy transfer resulting from a disparity in temperature is commonly referred to as heat. The field of research concerned with the analysis and understanding of heat transfer focuses on quantifying the rate at which this energy is exchanged. Heat is defined as the transfer of energy between two systems that occurs due to a difference in temperature when they interact. The field of heat transfer typically identifies three separate types of heat transport: conduction, convection, and radiation. The three modes under consideration exhibit similarities in that they all need the presence of a temperature differential and involve heat exchange occurring in the direction of decreasing temperature. Each approach exhibits distinct physical characteristics and is governed by unique governing principles (Shah & Sekulic, 2003).

1.1.1. Conduction heat transfer

When a temperature gradient is present inside a physical system, empirical evidence indicates that there is a flow of energy from the region with higher temperature

to the region with lower temperature. It is commonly acknowledged that energy transmission occurs through the process of conduction, whereby the rate of heat transfer per unit area is directly proportional to the temperature gradient perpendicular to the surface:

$$q_x = -kA \frac{\partial T}{\partial x} \tag{1.1}$$

Where q_x is the heat-transfer rate and $\partial T/\partial x$ is the temperature gradient in the direction of the heat flow. The positive constant k is called the thermal conductivity of the material, and the minus sign is inserted so that the second principle of thermodynamics will be satisfied; i.e., heat must flow downhill on the temperature scale. Equation (1.1) is called Fourier's law of heat conduction (Dewan et al., 2004).

1.1.2. Convection heat transfer

Convection refers to the process by which energy is transferred between a solid surface and a surrounding liquid or gas in motion. This mode of heat transfer encompasses the combined influences of conduction and fluid motion. There is a direct correlation between the speed of fluid motion and the magnitude of convection heat transfer. When there is no significant movement of fluid, the transmission of heat between a solid surface and the surrounding fluid occurs solely by conduction. The inclusion of fluid bulk motion serves to augment the heat transfer occurring between the solid surface and the fluid. However, it concurrently introduces complexities in the estimation of heat transfer rates. To express the overall effect of convection, we use Newton's law of cooling:

$$q = hA(T_w - T_\infty) \tag{1.2}$$

Here the heat-transfer rate is related to the overall temperature difference between the wall and fluid and the surface area A. The quantity h is called the convection heat-transfer coefficient. An analytical calculation of h may be made for some systems. For complex situations it must be determined experimentally. The heat-transfer coefficient is sometimes called the film conductance because of its relation to the conduction process in the thin stationary layer of fluid at the wall surface (Dewan et al., 2004).

1.1.3. Radiation Heat Transfer

Radiation refers to the release of energy by matter in the form of electromagnetic waves, commonly known as photons, which occurs due to alterations in the electronic configurations of atoms or molecules. In contrast to conduction and convection, the process of energy transfer through radiation does not necessitate the existence of an intermediary medium. In the field of heat transfer research, there is a focus on the phenomenon of thermal radiation, which refers to the emission of radiation by objects due to their respective temperatures (Dewan et al., 2004). This phenomenon has distinct characteristics in comparison to other types of electromagnetic radiation, namely x-rays, gamma rays, microwaves, radio waves, and television waves, which do not possess a direct correlation with temperature. It is a well-established scientific fact that all objects with a temperature greater than absolute zero have the ability to produce thermal radiation. Thermodynamic principles indicate that an ideal thermal radiator, sometimes referred to as a blackbody, will release energy at a rate that is directly proportional to the fourth power of the absolute temperature of the object and directly proportional to its surface area. Thus:

$$q_{\text{emitted}} = \sigma A T^4 \qquad\qquad (1.3)$$

where σ is the proportionality constant and is called the Stefan-Boltzmann constant with the value of 5.669×10^{-8} W/m^2. K^4.

1.2. Heat Transfer Enhancement Methods

There are a number of techniques about how to improve heat transfer, including the idea that increasing the surface area of the heat exchanger or the coefficient of thermal conductivity between the fluid and the surface will result in a more efficient heat exchange. Heat transfer enhancement, augmentation, or intensification refers to the process of boosting the efficiency of heat transmission. A heat exchange's convective heat transfer can be improved with the use of augmentation techniques by decreasing the exchanger's thermal resistance. Although the heat transfer coefficient improves when heat transfer enhancement techniques are used, the pressure drop also rises. Most commonly used heat transfer fluids are conventional fluids like water, ethylene glycol, and engine oil. There are many strategies for improving heat transmission, however traditional fluids' poor performance limits those possibilities.

Heat transfer enhancement methods so far, the bulk of research on heat transfer has concentrated on gaining an understanding of the process under normal conditions. Recently, the need for more efficient heat transfer systems has raised interest in and research into approaches that enhance or intensify heat transport (Warren, 1968). The laboratory evaluation of these methods has progressed to the point where a number of them may be assessed seriously for application to commercial heat-exchange equipment. These solutions enhance heat transfer, but often at the expense of higher pumping power, externally supplied power to the system, increased expenditures, and/or increased weight. Bergles and Morton (Bergles & Morton, 1965) provide a thorough analysis and assessment of these techniques. Establishing broadly applicable selection criteria for the employment of augmentative methods is one of the challenges. Given the number of variables involved in the choice issue, this looks to be an almost insurmountable challenge. In addition to economic considerations such as maintenance cost, development cost, etc., other aspects such as reliability and safety are also relevant.

Heat transfer between single- and multi-phase gases and liquids has been accomplished with the help of finned-tube heat exchangers. The barrier to heat transmission on the air side is what limits the efficiency of a finned tube heat exchanger. This is because the heat transfer coefficient from the air side to the liquid side is much smaller. Therefore, fins are employed to enhance the surface area of the gas side of the heat exchanger so that the thermal conductance on both sides are equal. Although elliptical tubes are less frequent, circular and rectangular tubes are still employed in tube-fin heat exchangers.

Figure 1.1. Longitudinal fins on individual tube (Shah & Sekulic, 2003)

1.2.1. Active heat transfer augmentation methods

These solutions are more complicated from an application and design standpoint since they need an external power input to achieve the necessary flow modification and increase in heat transfer rate. Electro-hydrodynamic enhanced boiling has gained a significant deal of interest from academic and industry researchers due to its increased potential for practical use. Refrigerants have been found to increase heat transfer coefficients by up to 900 percent during pool boiling.

The necessity to construct trustworthy, low-cost transducers or power supply and updated heat exchangers may limit the practical use of active techniques, notwithstanding their efficiency in lowering wall superheat and/or boosting the critical heat flux. These methods have not been as successful as passive ones since it is often difficult to offer external power input. The following are examples of active methods (Bergles, 1998):

1. Rotating or wiping the heat transfer surface mechanically.
2. Suction or injection the working fluids.
3. Surface vibration and fluid vibration.
4. Jet Impingement.

1.2.2. Passive heat transfer augmentation methods

The term "passive" refers to the fact that no additional energy is being added to the system; rather, the energy required to improve heat transfer is drawn from the system's total available energy. The loss of fluid pressure is an obvious drawback. The discussion in this section follows the paper by Jacobi and Shah (1998) and also a work by Webb (1987) and makes reference to a comprehensive summary of many basic design geometries and experimental data of Kays and London (1998). Essential to these tactics is the improvement of convective heat transfer, which may be achieved by the use of the following concepts (Adrian & Allan, 2003):

1. Reducing the thickness of the thermal boundary layer.
2. Increasing the disruption of fluid flow.
3. Enhancing the velocity gradient close to the heat transfer wall.

This approach creates turbulence in most fluids and breaks the actual boundary layer in order to enhance "the effective surface area, residence time, and therefore the heat transfer coefficient" in the current system. The passive technique is classified as (Bergles, 1998):

1. Treated Surfaces (Coating).

2. Extended Surfaces.

3. Displaced Insert Devices.

4. Swirl Flow Devices (Non-Movable).

5. Rough Surfaces.

6. Surface Tension Devices.

7. Additives for Liquids.

Figure 1.2. Full length twisted tape as a passive technique (Chintan et al., 2012)

1.2.3. Hybrid heat transfer enhancement methods

Recall that compound augmentation includes the simultaneous use of two (or more) approaches to achieve an enhancement that is greater than the sum of the enhancements produced by the individual techniques. This technique involves complex design and hence has limited applications (Bergles, 1998). Some examples of compound techniques are given below:

1. Rough tube walls with twisted tape.

2. Rough cylinder with acoustic vibrations.

3. Externally finned tube with Nano fluid.

4. Fins and electric fields.
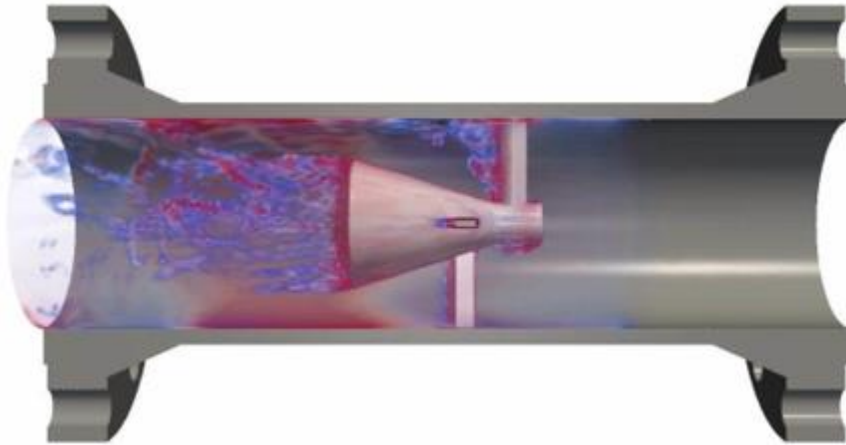
Figure 1.3. Acoustic induced vibration (Bergles, 1998)

1.3. Heat Exchanger Types

Heat exchangers are widely utilised equipment in several process sectors. Heat exchangers are utilised for the purpose of facilitating the transfer of heat between two distinct process streams. It is evident that the utilisation of a heat exchanger is necessary for every operation involving cooling, heating, condensation, boiling, or evaporation. Process fluids typically undergo heating or cooling prior to the commencement of the process or undergo a phase transition. Heat exchangers are classified based on their specific use. Heat exchangers that are utilised for the purpose of condensation are commonly referred to as condensers. Similarly, heat exchangers that are employed for boiling applications are commonly known as boilers. The performance and efficiency of heat exchangers are evaluated based on the quantity of heat transferred while minimising the heat transfer area and pressure drop. The evaluation of pressure drop and necessary surface area for a given heat transfer rate offers valuable information regarding the financial investment and operational energy consumption of a heat exchanger. Typically, a wealth of literature and theoretical frameworks exist for the purpose of designing a heat exchanger in accordance with specific specifications. There exists a wide variety of heat exchangers (Gupta, 1986).

1.3.1. Shell and tube heat exchanger

The shell and tube heat exchanger is a commonly used heat transfer device in applications with elevated pressures, typically reaching up to 552 bars. The heat exchanger under consideration is a shell and tube type, which falls into the category of indirect contact heat exchangers. The system is comprised of a sequence of conduits, within which a fluid is transported. The shell serves as the enclosure for the shell fluid.

In general, the object exhibits a cylindrical morphology characterised by a circular cross-sectional profile, however alternative shell geometries are employed in specialised contexts. This study focuses on the utilisation of a one-pass shell, also known as a shell, for the purposes of examination. The shell is widely utilised primarily because of its affordability and simplicity, and it exhibits the largest correction factor for the log-mean temperature difference (LMTD). While the tubes may possess either single or many passes, it is important to note that there is a singular pass on the shell side.
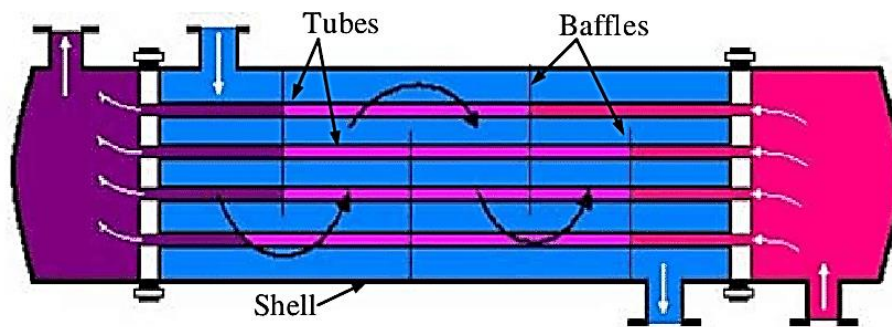
Figure 1.4. Shell and tube heat exchanger (Kakac & Lui, 2002)

Conversely, the other fluid circulates within the shell, passing over the tubes in order to facilitate the process of heating or cooling. The fluids on the tube side and shell side are physically segregated by means of a tube sheet (Kakac & Lui, 2002).

1.3.2. Welded plate heat exchangers

Welded plate heat exchangers are fabricated through the process of welding heat transfer plates onto both the hot and cold fluid streams of the apparatus. This welding technique offers a notable reduction in the overall cost associated with welding the complete plate. Laser welding is commonly employed to join the plates of a gasketed plate heat exchanger. The welding process occurs at the precise region where the gaskets are typically positioned. Furthermore, this welding procedure encompasses the entire diameter of the plat (Home - API Heat Transfer, 2023).

The utilisation of a welded plate heat exchanger is advantageous when handling corrosive fluid streams as either the hot or cold fluid media. This is due to the inherent resistance of the welded corrugated metal plates, which serve as the heat transfer media, against wear and tear caused by corrosive fluids. Welded plate heat exchangers are characterised by their compact size and robust construction, as they are designed without the need for gaskets. This feature enables them to effectively function under extreme temperature and pressure conditions. The materials employed in the production of the

plates encompass stainless steel, hastelloy, nickel-based alloys, titanium, and copper (Shah & Sekulic, 2003).
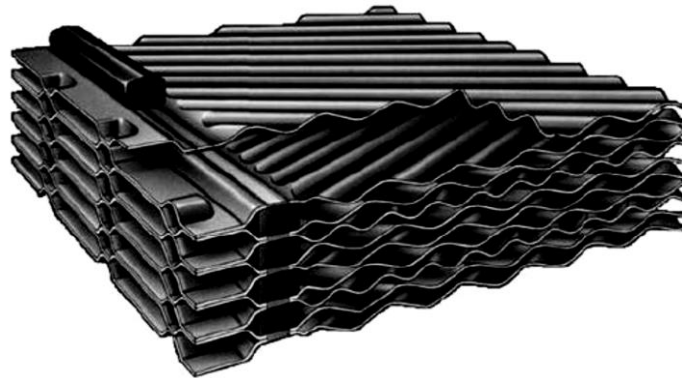
Figure 1.5. Plate section of a welded plate heat exchanger (Home - API Heat Transfer, 2023)

1.3.3. Lamella heat exchanger

The lamella heat exchanger consists of a series of parallel welded thin plates that, when arranged longitudinally within a shell, create a rectangular channel. The lamellas consist of paired thin flat plates that are typically equipped with gaskets in order to mitigate the occurrence of leakages. The utilisation of this particular plate heat exchanger is commonly observed in the pulp-paper and chemical process sectors for the purpose of reclaiming process heat. The operational pressures range up to 3.45 mega Pascal (MPa), while the temperature limitations fall within the range of 200 degrees Celsius to 500°C (Kakac & Lui, 2002).
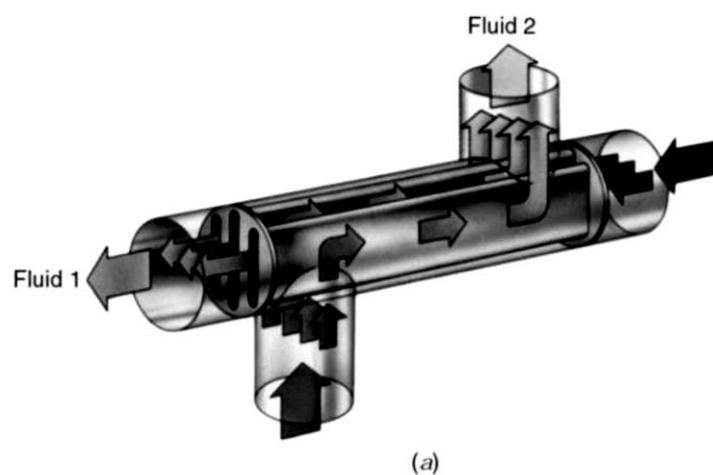
Figure 1.6. Cross section of the Lamella heat exchanger (Home - API Heat Transfer, 2023)

1.3.4. Finned tube Heat Exchanger

Using finned tube heat exchangers, gases and liquids in a single or two-phase system may be heated to different temperatures. The air side heat transfer resistance is what limits the finned tube heat exchanger's performance. Air-side heat transfer coefficients are much lower than liquid-side heat transfer coefficients.

On the gas side, fins are used to enhance surface area in order to achieve balanced thermal conductance on both sides for the smallest possible heat exchanger. However, elliptical tubes are also used. Fins are typically attached to the exterior of tubes, although they can also be installed on the interior. Tight mechanical fits, tension winding, adhesive bonding, soldering, brazing, welding, and extrusion are all used to secure them to the tubes. The following are the several types of tube-fin exchangers based on the type of fin they use:

1. Individually finned tube exchangers or tube exchangers with standard fins on individual tubes.
2. A tube–fin exchanger with continuous flat fins. The fins might be flat, undulating, or interrupted. The array of tubes may include tubes of various forms, including round, oval, and rectangular.
3. Longitudinal fins on individual tubes.

The highest temperature is limited by the type of bonding, materials employed and material thickness (Shah & Sekulic, 2003).

Figure 1.7. Finned tube heat exchanger (radiator) (Shah & Sekulic, 2003)

1.3.5. Double pipe heat exchanger

In a double-pipe heat exchanger, one smaller pipe is concentrically nested within another, larger pipe, and both pipes include end fittings to control the flow of fluids between the two pipes. Heat exchanger with two pipes is shown in Figure 1.4. In the

configuration depicted, the inner pipe of the heat exchanger carries the hot process fluid, which transfers its heat to the outside pipe, which carries the cooling water.
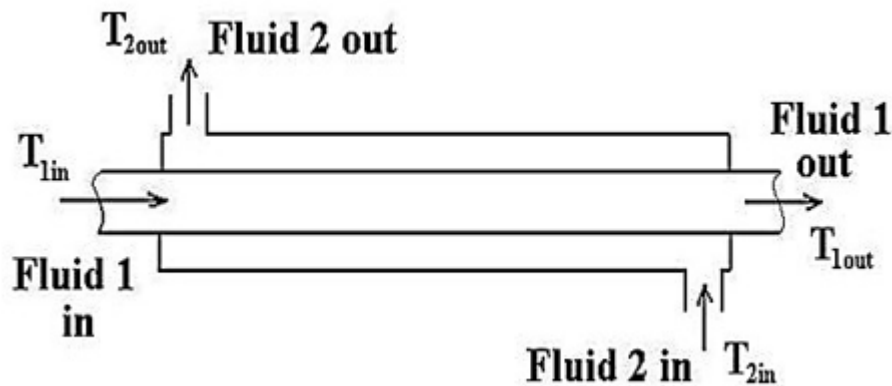
Figure 1.8. Diagram of counter-flow double pipe heat exchangers (Bright Hub Engineering, n.d.)

The double pipe heat exchangers are suited for applications that have relatively low flow rates and high temperature or pressure. Other uses are sensible heating or cooling of process fluids in applications where the heat transfer areas are small (up to 50 m^2). The main advantages of using double pipe heat exchanger are:

1. Piping arrangement Flexibility
2. Quick and easy to maintain using standard components
3. Can handle high pressures and temperatures.
4. Economically feasible and less deliveries compared to other heat exchanger due to its simple design and construction.

1.3.6. Double pipe heat exchanger applications

One major application of double pipe heat exchanger is in air cooled heat exchangers, atmospheric air, like all low pressure gases, gives a very low heat transfer coefficient at normal velocities. By contrast the tube- side fluid, usually a liquid to be sensibly cooled or a vapour to be condensed may have a coefficient up to 100 times higher, or even more. Therefore, double pipe heat exchangers are used in these exchangers to reduce the overall size of exchanger required. Even so, some of these installations cover several areas (Bell et al., 1984). The other applications are use in a variety of sensible, condensing, and boiling services and heat exchangers especially in shell and tube exchangers. A typical sensible heat transfer application would be cooling a compressed gas in a compressor inter-cooler, using cooling water in the tubes. Double

pipe heat exchangers are used for condensing organic vapours, which have condensing coefficient only a third or a quarter of that of the cooling water inside the tubes. In addition to providing additional heat transfer area, the fins provide drip points that facilitate the drainage of the condensate.

1.4. Nano fluid technology

The second way for improving heat transmission is Nano fluid technology. Nano fluid are a combination of base fluid and nanoparticles of metal suspended in suspension. Nanoparticles are particles with a diameter between 0.1 and 100 nm. Metal or metal oxide nanoparticles, such as Copper, Aluminum, and Titanium, are often found in Nano fluid. When mixing with nanoparticles, typically a conductive fluid such as water or ethylene glycol is utilized as the base fluid. This is because metals have a much higher thermal conductivity per unit volume than liquids, and therefore adding nanoparticles to a fluid increases its effective thermal conductivity and, as a result, its heat transfer rate. Above the base fluid, thermal conductivity rises by 15% on average, whereas heat transfer coefficient rises by 40%. Common oxide nanoparticles in heat transfer studies include "Zinc Oxide (ZnO), Copper Oxide (CuO), Aluminum Oxide (Al_2O_3), and Titanium Oxide (TiO_2)", whereas metal nanoparticles include "Gold (Ag), Silver (Au), and Copper (Cu)" (Emily, 2008).

Figure 1.9. Mixing of nanoparticles with base fluid (Emily, 2008)

1.4.1. Nanoparticle production

Nanoparticles may be produced by either a physical process or a chemical process. Both methods are possible. The mechanical grinding technique and the inert gas condensation method are both included in the physical procedures. Chemical

precipitation, spray pyrolysis, and thermal spraying are the processes that fall within the category of chemical processes (Emily, 2008).
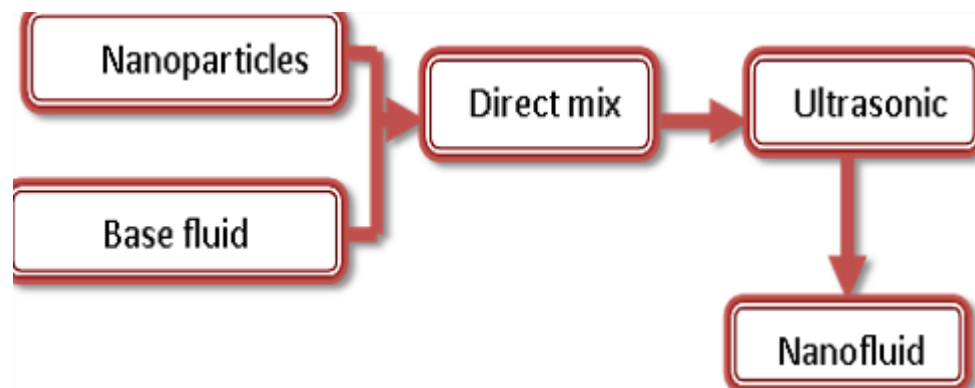
Figure 1.10. The preparation process of Nano fluid

1.4.2. Shape and size of particle

Typically, the diameter of nanoparticles employed in Nano fluid production is less than 100 nm. Particles might be spherical, rod-shaped, or tube-shaped. The particle size has a considerable impact on the heat transfer coefficient. The increase in the surface area of the nanoparticles that is exposed to heat transfer is responsible for the rise in the heat transfer coefficient that occurs when the size of the nanoparticles is decreased. The Nano fluid environment is dominated by the presence of spherical particles (Kevin, 2010).

1.4.3. Preparation of Nano fluid

The term "Nano fluid" does not only refer to the mixing of solid particles with a base fluid. In order to make Nano fluid by dispersing nanoparticles in base fluid, it is necessary to have a durable suspension, low or no agglomeration of particle, and no chemical change in the fluid itself. Furthermore, it is necessary to have precise mixing and particle stabilization (Kevin, 2010). In general, the stability of a suspension against the sedimentation of nanoparticles may be achieved using the following three methods:

1. Controlling the particle suspension's PH value.
2. Surface activator or surfactant additive.
3. Utilization of ultrasonic vibration.

Surfactants often employed in the manufacture of Nano fluids, such as "Cetyltrimethyl Ammonium Bromide (CTAB), oleic acid, and sodium dodecyl sulfate (SDS)", must be added without affecting the thermal characteristics of the Nano fluid. The choice of surfactant depends mostly on the solution and nanoparticle characteristics (Duangthongsuk & Wongwises, 2009).

Figure 1.11. Ultrasonic cleaner (Emily, 2008)

However, there are primarily two processes utilized to create Nano fluid:

1. Single-Step Process: The one-step process simultaneously generates and disperses nanoparticles in the base fluid, similar to the direct evaporation method developed by (Duangthongsuk & Wongwises, 2009), and consists of a fluid-carrying revolving cylinder. A source material is vaporized in the middle of the cylinder. When the vapor touches the cooled liquid, it condenses seen in Figure 1.9. However, this method has limitations in that it can only create a small amount of product and low vapor pressure liquids must be used. Another single-step technique, "Submerged Arc Nanoparticle Synthesis System (SANSS)", was created to create evenly distributed CuO nanoparticles in a dielectric liquid (deionized water).
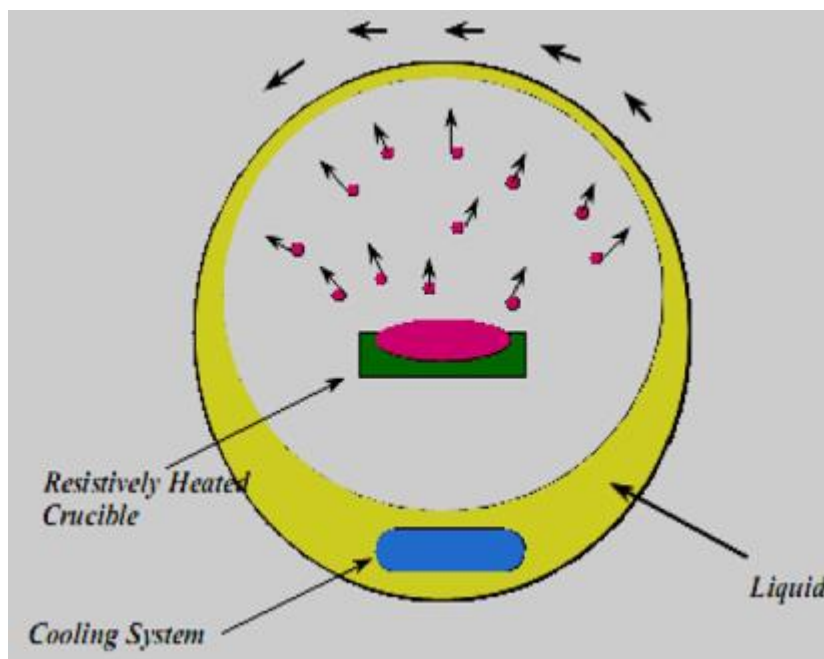
Figure 1.12. One step Nano fluid preparation (Duangthongsuk & Wongwises, 2009)

In concept, the approach generates a stable Nano fluid consisting of a copper rod immersed in a dielectric liquid in a vacuum chamber. An appropriate electric power source is utilized to create an arc between 6,000 and 12,000 degrees Celsius, which melts and vaporizes the metal rod in the location where the arc was formed. Simultaneously, the arc evaporates the deionized water. The vaporized metal passes through nucleation, growth, and condensation, culminating in the dispersion of nanoparticles in deionized water. It was possible to produce Nano fluids with CuO particles measuring 38.9 ± 49.1 nm (Lee et al., 1999).

2. Two-Step Process: Considering the commercially accessible Nano powder offered by a number of firms, its application in the manufacture of Nano fluid is widespread. In this approach, nanoparticles were generated and subsequently disseminated throughout the base fluids. In general, ultrasonic equipment is used to scatter particles extensively and decrease particle agglomeration as compared to a single-step procedure. The two-step technique works effectively with oxide nanoparticles but less so with metallic particles unless ultrasonic equipment is used (Lo et al., 2005).

Ultrasonic equipment It may be used to pulverize animal and plant cells, viruses, germs, and tissues, in addition to reshaping inorganic material. It is also applicable for emulsification, separation, distribution, collection, cleaning, and Nano-material preparation. In general, procedures such as adjusting the PH value, adding a dispersion, and using ultrasonic vibration are used to generate stable suspensions by altering the surface characteristics of suspended particles and preventing the development of particle clusters.

1.4.4. Cluster and agglomeration of Nano fluid

One of the main difficulties in micro fluid investigations was the quick settling of nanoparticles. Although studies show that incorporating nanoparticles into a fluid considerably improves its thermal conductivity, advancements in actual applications have been slowed. Particles settling on surfaces and plugging micro channels both reduced the total heat transfer of the fluid (by reducing the effective surface area utilised for heat transfer).
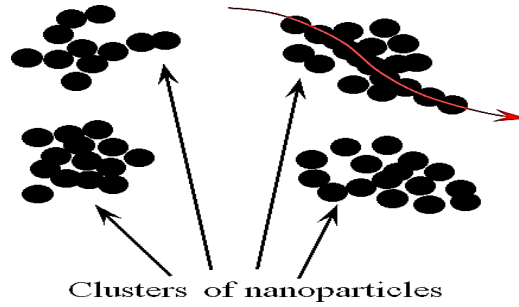
Figure 1.13. Schematic representation of nanoparticle cluster and their phenomenon

Even though nanoparticles drastically cut down on agglomerated particles, the issue still arises, especially at concentrations above 5%, and can hamper the heat conductivity of the Nano fluid. Because oxide nanoparticles require a higher volume concentration to provide the same gain in heat conductivity as metallic nanoparticles, agglomeration is more apparent when using oxide nanoparticle (Wen & Ding, 2004). As a consequence of Van der Waals forces, particles tend to clump prior to dispersion in a fluid. This is particularly apparent in metallic particles, since dipoles may rapidly form in their molecules. The production of dipoles increases the attraction between neighboring dipoles. These dipoles, which may exist even in neutral particles, are the origin of Van der Waals forces. It is considered that this attraction force is the principal source of particle aggregation, especially in Nano powders. To solve this challenge, several manufacturing and dispersion strategies for nanoparticles in fluids have been proposed. The addition of surface treatments to nanoparticles is one option, while other ways have been employed to reduce particle clusters. Typically, these techniques include agitating the Nano fluid to separate clusters into individual particles and avoid sedimentation (Duangthongsuk & Wongwises, 2008). Clustering phenomena are seen in Figure 1.10.

1.4.5. Volume concentration (φ)

Volume concentration refers to the ratio of nanoparticles to the overall volume of Nano fluid. This ratio is very important in Nano fluid application because all physical properties of Nano fluid dependent on this ratio such as (thermal conductivity, specific heat, density, and viscosity) (Emily, 2008).

1.4.6. Application of Nano fluid

Due Many applications can benefit from using Nano fluid because of their superior heat transmission and thermos-physical properties. When it comes to heat

transfer, Nano fluid have the most significant uses. One appealing property of Nano fluid is their high thermal conductivity. It's a measure of how well a substance transfers heat. The measurement of Nano fluid thermal conductivity has been the subject of extensive study. It has been shown that, in comparison to base fluids, Nano fluid offer superior heat conductivity. Nano fluid is used in many different kinds of manufacturing, including:

1. Industrial cooling application

By using Nano fluid for cooling purposes in industry, significant energy savings and emission reductions may be possible. Using Nano fluid in closed loop cooling cycles in the U.S. electric power industry might save roughly 10-30 trillion Btu annually, and replacing cooling and heating water with Nano fluid has the potential to save 1 trillion Btu of energy for U.S. industry (Yu et al., 2008).

2. Nuclear Reactors

MIT's nuclear science and engineering group studied the potential of Nano fluid in the nuclear industry by looking at how they could improve the efficiency of water-cooled nuclear power plants that are limited by heat removal. Pressurized water reactors (PWRs) could employ it as their primary coolant, secondary safety systems, accelerator targets, plasma diverters, etc.
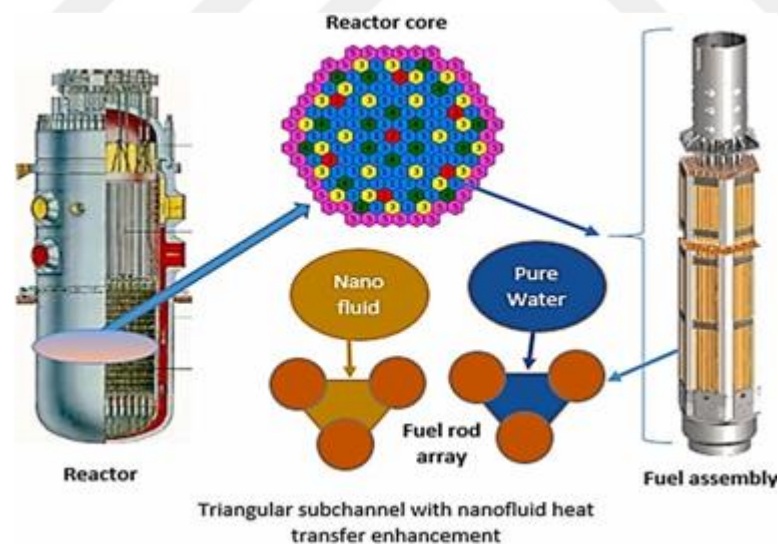
Figure 1.14. Alumina Nano fluid as a coolant in a hexagonal rod-bundle reactor core (Yu et al., 2008)

3. Electronic applications

A Nano fluid used to cool microchips in computers and other electronic devices. Microfluidic uses, such as the cooling of microchips, are being used in other electronic applications.

Figure 1.15. Nano fluid as a coolant in electronic devices (Yu et al., 2008)

Rapid heat dissipation is a significant barrier to the miniaturization of microchips. Nevertheless, owing to their great thermal conductivity, Nano fluid may be employed to liquid-cool computer chips. It is anticipated that the next generation of computer processors would generate a localized heat flux more than 10MW/m^2 and a total power greater than 300W (Yu et al., 2008).

1.5. Objective of The Thesis

There appears to be a need for more research on the impact of nanotechnology applications in finned tube heat exchangers on thermal performance. The primary goal of this study is to use numerical methods to calculate the pressure drop and heat transfer characteristics of double-pipe (Annular) heat exchangers, as well as to analyze the impact of heat exchanger geometry and Nano fluid properties on these variables. The following specific aims were pursued towards this end:

1. Design and construction of a physical model of the heat exchanger.
2. Development of a numerical model of the heat exchanger using commercial CFD's Package (Ansys fluent).
3. Testing of the physical model under different flow rates and configuration (counter- flow).
4. Evaluation the heat transfer enhancement ratio due the heat transfer augmentation technique used.
5. Make an optimization to find the best configuration of heat transfer used.
6. Comparison of the results from numerical work with the published results.

1.6. Importance of the Thesis

The extensive use of finned tube heat exchangers is widely documented in the public domain. Most studies, however, have contrasted the efficiency of finned and smooth tubes in order to determine the impact of variables like fin height, fins spacing, thickness, tube diameter, fin density, and fin type (plate, integral, pins, etc.). With regards to the longitudinal finned tube heat exchangers, there are some researches which are presented for optimization the fin shape experimentally and numerically. It seems that nanotechnology applications in finned tube heat exchangers need additional investigations to probe the effect of this technology on its thermal performance. Fins improve heat transfer significantly, which is a major benefit. But their growing bulk, expense, and weight are all drawbacks. Reducing all these drawbacks while increasing heat transmission would be highly beneficial. Nano fluid are the better technique to overcome these disadvantages. By adoption Nano fluid, thermal performance of heat exchanger can be improved and at same time the surface area will be reduced. The focus of this study is to investigate the performance of a U-longitudinal finned tube heat exchanger and compare it with a smooth tube heat exchanger. Subsequently, the performance of the system with Nano fluids will be examined. The process involves the incorporation of nanoparticles into a base fluid. This study aims to investigate the impact of the newly developed technology on the estimated decrease in the surface area of fins.

As a matter of fact, increased heat transfer surfaces can be put to use in a number of contexts. Heat exchangers can be made smaller and cheaper with the use of improved surfaces. They also reduce the amount of pumping power needed for particular heat exchange operations. They also improve heat exchangers by increasing their UA, which allows for a lower mean temperature differential or a higher heat exchange rate for a given fluid inlet temperature. This, in turn, increases the efficacy and efficiency of thermal processes while decreasing operating costs. In order to enhance the thermos-hydraulic efficiency of heat exchangers, efforts have been made by the industry to augment thermal contact by increasing the heat transfer coefficient, while simultaneously reducing the power required for pumping.

2. LITERATURE REVIEW

Heat transfer improvement techniques have recently been implemented in a wide variety of industrial applications, including the refrigeration, automotive, and process sectors, with positive results. There may be a number of monetary and ecological benefits to enhancing heat transmission in heat exchangers. Materials, energy, and money are all saved thanks to compact and efficient heat exchanger designs.

This literature review will focus on the most important issues. Due to its increasing prevalence in a wide range of industrial settings, the finned tube has been the topic of numerous research efforts. The improvement in heat transfer by using a finned tube in all applications will be discussed, as will "the influence of designs for heat exchangers: e.g., transverse tube spacing, longitudinal tube spacing, tube diameter, number of tube rows, fins spacing or fins density, fins height, fins thickness, and type of fins," all of which will be examined in detail in this literature review.

2.1. Heat Exchanger Experimental Studies

The study conducted by Prabhanjan et al. (2002) examined the heat transfer rates of a straight tube heat exchanger and a helically coiled heat exchanger, aiming to compare their performance. The objective of this study was to assess the comparative benefits of employing a helically coiled heat exchanger in contrast to a straight tube heat exchanger for the purpose of liquid heating. The majority of research endeavours concentrate on either maintaining a constant wall temperature or a constant heat flux. The findings of these studies indicate that the heat transfer coefficient is influenced by both the heat exchanger's geometry and the temperature of the water bath encompassing the heat exchanger. The experiments were conducted within the transitional and turbulent flow regimes. The utilisation of a helical coil heat exchanger was observed to result in an enhanced heat transfer coefficient in comparison to a straight tube heat exchanger with similar dimensions. The temperature increase of the fluid was observed to be influenced by both the coil geometry and the flow rate. The heat transfer coefficients of both heat exchangers exhibited an increase when the temperature of the bath was raised.

Naphon and Wongwises (2002) conducted experimental investigations to determine the convective heat transfer coefficients within the tube of a spiral coil heat exchanger. The test part comprises a heat exchanger in the form of a spiral coil, consisting of six layers of concentrically arranged spiral coiled tubes. The fabrication process involves the bending of a straight copper tube with a diameter of 9.27 mm into a spiral

coil comprising five turns. The experiments are conducted in circumstances with reduced humidity. The experimental data are juxtaposed with the calculated values derived from correlations established in previous investigations. Furthermore, this study presents a novel correlation for the determination of in-tube heat transfer coefficients in the context of spirally coiled tubes utilised in dehumidifying scenarios. This correlation is intended to be applied in practical settings. The correlation is as follows:

$$Nu_{\text{ave}} = 27.358 De^{0.287} \text{Pr}^{-0.949} \tag{2.1}$$

For: De $\geq$ 300, Pr $\geq$5

An experimental investigation by Salimpour (2008) was performed to study the heat transfer characteristics of temperature dependent-property engine-oil inside shell and coiled tube heat exchangers. For this purpose, a well instrumented set-up was designed and constructed. Three heat exchangers with different coil pitches were selected as the test section for counter-flow configuration. Engine-oil was circulated inside the inner coiled tube, while coolant water flowed in the shell. From the results of this study, it was found out that the increment of oil inlet temperature decreases the heat transfer coefficients. Also, it was seen that the coil-side heat transfer coefficients of the coiled tubes with larger pitches are less than those of the ones with smaller pitches; and the effect of pitch on Nusselt Number is more discernible in high temperatures. Finally, based on the results of this study, a correlation was developed to predict the coil-side heat transfer coefficients of the shell and coiled tube heat exchangers:

$$Nu_i = 0.554 De^{0.496} \gamma^{-0.388} \text{Pr}^{-0.151} \phi^{0.153} \tag{2.2}$$

Salimpour (2009) conducted experimental investigations on the heat transfer coefficients of shell and helically coiled tube heat exchangers. Three heat exchangers featuring distinct coil pitches were chosen as the experimental units for evaluating both parallel-flow and counter-flow arrangements. The necessary parameters, such as the intake and outlet temperatures of the fluids on the tube-side and shell-side, as well as the flow rate of the fluids, are all required. The study's findings indicate that the shell-side heat transfer coefficients of coils with bigger pitches are greater than those of coils with smaller pitches. Also based on the results of this study, two correlations were developed to predict the inner and outer heat transfer coefficients of the coiled tube heat exchangers the following correlation as:

$$Nu_i = 0.152De^{0.431}Pr^{1.06}\gamma^{-0.277} \tag{2.3}$$

$$Nu_o = 19.6Re^{0.513}Pr^{0.129}\gamma^{0.983} \tag{2.4}$$

Conté & Peng (2009) conducted both computational and experimental investigations in order to gain insights into the convective heat transfer phenomenon emanating from a single round pipe coiled in a rectangle pattern. The heat exchangers under investigation consist of both inner and outside coils, resulting in an external flow pattern that closely resembles the flow within tube-bundles. The heat exchangers consist of both inner and outside coils, which are comprised of sections that include bends and straight segments. Calculations and experiments were conducted to investigate two distinct scenarios characterised by varying external flow configurations. The findings demonstrated that the impact of geometric arrangement on heat transfer was more favourable for Case 1, namely the staggered design. This may be attributed primarily to the more convoluted flow characteristics and improved mixing of the external fluid. The numerical and experimental findings exhibit a strong qualitative agreement. The findings from both numerical simulations and experimental investigations indicate that the act of coiling a pipe, so causing an external fluid to flow over or within a tube bundle, can effectively create turbulence without necessitating an increase in velocity.

Heat transfer characteristics of a new helically coiled crimped spiral tube heat exchanger were studied analytically by Kwanchanok & Wongwises (2008). The present work aims to experimentally evaluate the heat transfer properties in dry surface circumstances of a novel heat exchanger design, specifically a helically coiled finned tube heat exchanger. The construction of each tube involves the process of bending a straight copper tube into a helical coil. Helically arranged around the copper tube are aluminium crimped spiral fins, possessing a thickness of 0.5 mm and an outer diameter of 28.25 mm. The inner diameter of the fin has corrugations along its margin. The shell side use ambient air as the working fluid, while the tube-side utilises hot water. The experimental trials are conducted using air mass flow rates that vary from 0.04 to 0.13 kg/s. The water mass flow rates range from 0.2 to 0.4 kg/s. The water temperatures range from 40 to 50 °C. The results were There is no effect of air mass flow rate on the tube-side heat transfer coefficient, the inlet-water temperature and water mass flow rate show a significant effect on the out-side heat transfer coefficient, the effectiveness are inversely proportional to

air-side Reynolds number, but directly proportional to the water mass flow rate and inlet water temperature.

Experimental study of mixed convection heat transfers in vertical helically coiled tube heat exchangers were investigated by Ghorbani et al. (2010). This study aimed to experimentally explore the mixed convection heat transfer in a coil-in-shell heat exchanger. The investigation focused on various Reynolds numbers, tube-to-coil diameter ratios, and variable dimensionless coil pitch. The studies were done to investigate the characteristics of both laminar and turbulent flow within a coil. The increase in coil surface area was found to have a detrimental impact on heat transfer coefficient, leading to a fall in its value. In contrast, an increase in coil pitch leads to an augmentation in the convection heat transfer coefficient on the shell-side. The overall heat transfer coefficient of a heat exchanger exhibits a positive correlation with the heat transfer rate. Extensive investigations have been conducted on various attributes of the heat exchanger in order to determine the optimal characteristic length that establishes the relationship between the Nusselt number and the Rayleigh and Reynolds numbers. This relationship may be expressed as follows:

$$Nu_{Dh} = 0.0013 Ra_{Dh}^{0.5128} \text{Re}_{Dh}^{0.2} \text{Pr}^{0.3} \tag{2.5}$$

The experimental investigation conducted by Nasser et al. (2010) focused on examining the thermal performance of shell and heat exchangers. This work presents an experimental inquiry into the mixed convection heat transfer occurring in a coil-in-shell heat exchanger. The analysis encompasses several combinations of Reynolds and Rayleigh numbers, varied ratios of tube-to-coil diameter, and dimensionless coil pitch. The objective of this study was to evaluate the impact of tube diameter, coil pitch, shell-side mass flow rate, and tube-side mass flow rate on the performance coefficient and modified effectiveness of vertical helical coiled tube heat exchangers. The calculations have been executed to determine the steady-state conditions, while the experiments were carried out to investigate both laminar and turbulent flow phenomena within the coil. The study revealed that the ratio of mass flow rate from the tube-side to the shell-side had a significant impact on the axial temperature profiles of the heat exchanger. The findings further demonstrate that the relationship between the Effectiveness-Number of Transfer Units (ε-NTU) for the mixed convection heat exchangers is identical to that observed in a pure counter-flow heat exchanger.

2.2. Heat Exchanger Numerical Studies

Mirgolbabaei et al. (2011) conducted a numerical study to investigate the forced convection heat transfer from vertical helically coiled tubes. The study examined the effects of different Reynolds and Rayleigh numbers, varied coil-to-tube diameter ratios, and non-dimensional coil pitches. The researchers observed that as the dimensionless coil pitch in the medium range increases, there is a decrease in the heat transfer coefficient. Conversely, when the pitch is extended to 2 times the tube diameter, there is an increase in the heat transfer coefficient. Furthermore, it has been determined that the heat transfer coefficient falls as the tube diameter increases, while maintaining the same dimensionless coil pitch. Various characteristic lengths were employed in the computations of the Nusselt Number in order to ascertain the most suitable length that aligns with the data. Ultimately, it has been demonstrated that the normalised length of the shell-side of the heat exchanger adequately represents the desired location.

Rahul (2009) has conducted a study on the establishment of a correlation for the heat transfer coefficient in a concentric helical coil heat exchanger. The focus of this study pertains to the development of a correlation that characterises the heat transfer coefficient for a flow occurring between concentric helical coils. The current state of affairs The observed correlation exhibits significant deviations from the experimental findings as the spacing between the concentric coils increases. The experimental data and computational fluid dynamics (CFD) simulations conducted with Fluent 6.3.26 were utilised to establish an enhanced correlation for the heat transfer coefficient on the flue gas side of the heat exchanger. A mathematical model is formulated in order to analyse the data acquired from computational fluid dynamics (CFD) simulations and experimental findings. A comprehensive analysis has been conducted on a diverse dataset encompassing a broad spectrum of Reynolds numbers, ranging from 20,000 to 150,000. The equation (2-6) can be subject to large error due to the extreme range of data, as determined by the ratio of coil gap to tube diameter. The validity of the established equation is contingent upon the given ratio (Coil gap/ Tube diameter) falling within the range of 0.55 to 2.25. This encompasses a significant portion of the practical spectrum in which helical coil heat exchangers are commonly employed.

$$Nu = 0.02652604 Re^{0.834694285} Pr^{0.3} (\text{Gap -ratio})^{-0.096856199} \qquad (2.6)$$

Sami et al. (2013) employed Computational Fluid Dynamics (CFD) modelling to examine and evaluate the impact of Parabolic-Cut Twisted tape (PCT) inserts installed within a circular tube on the rate of heat transmission. They conducted simulations and analyses to predict this phenomenon. The simulation was conducted using a commercial computational fluid dynamics (CFD) software tool, specifically FLUENT-6.3.26. The circular tube under consideration in the model is characterised by a constant heat flux and exhibits laminar flow. The simulation involved the consideration of three distinct twist tapes, each with varying twist ratios (y=2.93, 3.91, and 4.89) and cut depths (w=0.5, 1, and 1.5 cm). The investigation revealed that the Nusselt number and friction factor in the tube equipped with PCT exhibit an upward trend when the twist ratios (y) and cut depth (w) decrease. The computational fluid dynamics (CFD) simulations yielded findings that aligned with the literature correlations for plain tubes, thereby validating the accuracy of the predictions. The observed discrepancies were found to be within a range of less than ±8% for the Nusselt number and ±6.5% for the friction factor.

Lishan (2002) carried out a numerical study to predict the temperature distributions and velocity profile of a circular tubes fitted with twisted-tape inserts in laminar fully developed flow region. The swirl flow was simulated by following the helically twisted flow path in the partitioned tube represented by a semi-circular cross-section geometry using the finite volume method. All cases study was studied, under uniform wall temperature (UWT) and uniform heat flux (UHF) boundary conditions. Numerical results for the variations in the velocity and temperature distributions with flow rate and twist ratio were of the twisted tape presented; the temperature distributions also reflected the influence of fluid Prandtl number Pr. The flow field created by twisted tape has a distinct pattern consisting of a solitary longitudinal vortex that undergoes a division into two helical vortices revolving in opposite directions. This division occurs as the Reynolds number (Re) increases or the twist ratio decreases. Both the pressure drop and heat transfer coefficient see significant increases.

Eiamsa-ard et al. (2009) presented numerical simulation of the swirling flow in a tube fitted with loose-fit twisted tape insert. Influence of the clearance ratio (CR= 0.0 (tight-fit), 0.1, 0.2 and 0.3) on Nusselt number, pressure drop and thermal index were numerically investigated at different tape twist ratios (2.5 and 5.0). The simulation was conducted under constant wall temperature conditions in the turbulent flow regime for a various range of Reynolds number ranging from 3000 to 10,000. k–ε turbulence model was used to solve the Navier–Stokes equation in common with the energy equation. It is

visible that the twisted tape inserts for twist ratio =2.5 with CR=0.0 (tight-fit), 0.1, 0.2 and 0.3 can enhance the heat transfer rates up to 73.6%, 46.6%, 17.5% and 20%, respectively and increase friction factors up to 330%, 262%, 189%, and 160%, respectively, as compared to the smooth tube. The tube with loose-fit twisted tape inserts with CR=0.1, 0.2 and 0.3 provided heat transfer enhancement around 15.6%, 33.3% and 31.6% lower than those with CR=0.0.

Masoud et al. (2009) conducted experimental and numerical investigation to find the pressure drop, heat transfer coefficient and thermal performance index of a circular tube fitted with the typical and three modified twisted tape inserts. In experimental part, the three modified twisted tape, like perforated, notched and jagged were used so as to compare their performance with the typical twisted tape. All inserts had a width of 15 mm, a pitch length of 5 cm and a twist ratio of 2.94. In numerical part, a 3-D numerical simulation was conducted by using the computational fluid dynamic code FLUENT6.2. The modeling was achieved so as to validate and explain the experimental observations. The results revealed that the heat transfer coefficient and thermal performance ratio of the jagged insert were higher than the other types. A maximum increase of 31% and 22% were observed in the Nusselt number and the thermal index, respectively as compared with those obtained for the typical twisted tape.

2.3. Finned Tube Heat Exchangers Studies

Finned–tube heat exchangers are widespread devices which are used in myriad applications. They have complicated performance characteristics. This literature survey aims to review part of the researches which were dealt with this subject theoretically and experimentally in the following paragraphs.

Wang et al. (1998) Achieved equivalent results with eight finned-tube heat exchangers. They determined that fin pitch had no influence on the heat transfer performance of four-row coils with (Re =1000). However, when (Re=1000), the performance of heat transmission is greatly reliant on fin pitch. For two-row configurations with decreasing fin pitch, an increase in heat transfer performance was observed.

Mon and Gross (2004) calculated the parameters of heat transfer and pressure drop on the air side of annular-finned tube heat exchangers numerically. Researchers studied the impact of fin spacing on four-row tube bundles with annular fins in staggered and in-line designs. Local heat transfers and flow properties of annular-finned tube bundles are

influenced by fin spacing to fin height ratio, and the boundary layer that forms on the fin and tube surfaces is reliant on this ratio. After the height ratio was increased to 0.32, the heat transfer coefficient of the staggered layouts remained unchanged. For both arrays, as the height ratio grew, the heat transfer coefficient increased across the entire measured range and the pressure drop decreased. Experimental correlations with respect to heat transmission revealed a high degree of concordance.

Sahiti et al. (2005) conduct an experimental study to learn how pin fins might improve heat transfer. Putting tiny cylindrical pins on the heat exchanger's surface proved to be a game-changer. The elements influencing the improvement of heat transmission were revealed by means of an equation based on elementary relationships between convection and conduction heat transfer. Using a pin element instead of a smooth tube heat exchanger, they were able to raise the Nusselt number in their study.

An integrated pin-fin tube heat exchanger was simulated in three dimensions by Shuai and Chang (2011) using fluid software. They proved that the software could successfully simulate integral pin-fin tubes numerically. It has been demonstrated that fluent software is a valuable tool for the design and development of heat exchange tubes due to its ability to do numerical simulations on integral pin-fin tubes.

Ayad (2011), the heat transfer characteristics of cross-flow air-cooled single-tube multiple passes (smooth and integrated low finned tube) and its impact on heat transfer enhancement were investigated. As test parts, two lengths of Perspex conduit were specified. Each test section is fitted with an eight- or four-pass test tube (single aluminum tube multiple passes). The test results demonstrated that the integrated low finned tube had a larger air side heat transfer coefficient than the smooth tube. Using the integrated low finned tube, the enhancement ratio for eight and four passes was (1.86 to 2.38).

The effect of perforated circular finned tubes on convective heat transfer in circular finned tube heat exchangers was studied by Dong et al. (2012). The pressure drop increased by 0.68 and 2.08 percent for the 2 hole and 4 hole samples, respectively, while the convective heat transfer coefficient increased by 3.55 and 3.31 percent.

Mon (2003) calculated mathematically how well circular finned-tube cross flow heat exchangers performed in terms of heat transfer and pressure decrease on the air side. Different finning geometries and row counts were investigated numerically. Additionally, efforts were undertaken to confirm the most beneficial tube design. The following were the study's pertinent qualitative results about the finning geometry:

1. The fin height effect for both tube arrays is in good agreement with the experimental data, whereby an increase in fin height results in a reduction in the heat transfer coefficient and an increase in the pressure drop.

2. The impact of the fin spacing is mostly dependent on the boundary layer associated with the air velocity; the effect of the fin spacing on the heat transfer coefficient is negligible when the boundary layers between the fins are diverging for the staggered array. For the in-line array, the larger spacing shows the greater rate of heat transmission.

3. The heat transfer coefficient and pressure drop of the staggered tube bank have astonishingly little effect on the change in fin thickness. Therefore, it is shown that the impact of fin thickness is minimal.

Yonghan Kim and Yongchan Kim (2005) conducted an experimental investigation of the optimal layout for large-fin-pitch flat-plate finned-tube heat exchangers. Twenty-two heat exchangers were tested, with modifications made to their fin pitch, number of tube rows, and tube alignment. The air-side heat transfer coefficient decreased as the number of tube rows was increased and the fin pitch was decreased. The heat transfer coefficient of the four-row heat exchanger coil dropped by about 10% as the fin pitch decreased from 15.0 to 7.5 mm across the Reynolds number range of 500 to 900 that was determined based on the tube diameter. Heat transfer coefficients decreased from 1 to 4 tube rows for all fin pitches. The heat transfer performance was over 10% better with the staggered tube alignment than with the inline alignment.

Halici and Taymaz (2005) Examined experimentally the influence of tube regulation space on heat and mass transfer and friction factor for aluminum fin and copper tube heat exchangers. The external surface heat transfer coefficient, the Colburn factor, and the friction factor were computed using a computer program and experimental data. The findings demonstrated that when the tube row spacing decreased, the external surface heat transmission and friction factor increased on the dry surface. Comparing wet and dry surfaces reveals that the Colburn factor and friction factor are greater for wet surfaces.

Theoretical and experimental investigations of the effects of different fin spacing on the heat transfer coefficient and fin efficiency in natural convection were conducted by Chen and Hsu (2007). Researchers combined the effects of radiation and convection into a single calculation of heat transfer coefficients. This circular fin was predicted to have a non-uniform heat transmission coefficient due to its annular shape. The entire annular circular fin was divided into a number of sub-fin sections so that the average heat

transfer coefficient and fin efficiency could be predicted based on ambient temperature, tube temperature, and fin temperature readings at a number of defined measurement locations. The results showed that the average value of the heat transfer coefficient increased with increasing fin spacing (S), while fin efficiency dropped.

Later and his team (2008) Fin efficiency and heat transfer coefficient on a circular fin in forced convection were explored theoretically and empirically for different fin spacing. Using a non-uniform assumption about the distribution of the heat transfer coefficient on a fin, sub- fin sections were built in order to determine the average heat transfer coefficient and fin efficiency. The results suggested that the effect of fin spacing (S) on the average value of the heat transfer coefficient may be negligible if S exceeds 0.018 m. The average heat transfer coefficient value increased with increasing the air speed "Vair for 1 m/s ≤ Vair ≤ 5 m/s (1550 ≤ Red ≤ 7760) and increasing the fin spacing for 0.005 m ≤ S ≤ 0.018 m. The fin efficiency value decreased with increasing Vair for 1 m/s ≤ Vair ≤ 5 m/s and seemed to be not very sensitive to the fin spacing".

Nagarani and Mayilsamy (2010) tested and analysed the heat transfer rate and efficiency of annular fins of both circular and elliptical shapes in a variety of environments. The elliptical fin was deemed to be superior to the circular fin. Heat transfer coefficients vary depending on location, time, flow conditions, and fluid properties. The heat transfer coefficient and the efficiency are both sensitive to variations in temperature and humidity.

The ideal longitudinal fins on the outer surface of the inner pipe in laminar and fully developed flow with uniform heat flux are investigated by Lqbal et al. (2013). At first, fins had a triangular profile. It was discovered that the number of fins, the ratio of radii, the number of control points, and the characteristic length all have a role in determining the optimal fin form. Nusselt numbers increased by 138%, 312%, and 263% for trapezoidal, triangular, and parabolic geometries of same diameter, and by 212%, 59%, and 90% for hydraulic diameter, respectively.

2.4. Double Pipe Heat Exchangers Studies

Suxin Qian et al. (2017) presented an analysis of the fundamental concepts, characteristics, and significant distinctions among regeneration techniques employed in different conventional cooling systems. This study aims to demonstrate the categorization of regeneration methods into three distinct types: the recuperative type, applicable to steady-state operating systems; the regenerative type, suitable for systems operating

under cyclic operation; and the heat recovery type, designed for systems utilising solid-state functional materials. This paper provides an analysis of the three different techniques of regeneration, including an examination of their underlying physical principles, a comprehensive overview of their current development status, and an evaluation of their respective advantages, limits, and distinctive characteristics.

Bejan et al. (2016) conducted an analysis of the flow architecture in a counter flow heat exchanger with the incorporation of a plenum at both ends of the core. In this configuration, the thermal resistance reaches its minimum value. This conclusion is applicable to both fully formed laminar flow and turbulent flow within the core.

Han Xiaoxing et al. (2018) conducted an examination of a novel concentric tube heat pipe heat exchanger. The device was specifically engineered and intended for use in integrated waste heat recovery systems, with the primary objective of achieving enhanced heat transfer efficiency when operating at lower temperature heat sources. The results indicate that the heat exchanger's performance in terms of heat transfer was improved when certain parameters were set. Specifically, when the evaporator length was 260 mm, the inclination angle was 60 degrees, the cooling water flow rate was 0.5 m^3/h, and the cooling water temperature was 30 degrees Celsius. Under these conditions, the heat exchanger achieved a maximum heat transfer quantity of approximately 1600 W, with an average thermal resistance of 0.042 degrees Celsius per Watt

The thermal performance and fluid characteristics of counter flow heat exchangers (CFHEs) were investigated by Piroozam et al. (2018). This simulation investigates the influence of parameters and solves the CFHEs unilaterally through the implementation of diverse numerical techniques. It has been determined that the use of certain methods will enhance the performance of the CFHEs.

Verma etal. (2017) hypothesised about the thermal performance of a heat exchanger by examining the effects of several pipe surface shapes, including non-corrugated and corrugated pipes. The pitch and depths of corrugated pipe exhibit variation. The highest heat transfer coefficient is obtained by using helical-shaped ribs with a pitch of 4 mm and a depth of 1.5 mm. This configuration was tested at various Reynolds numbers ranging from 5000 to 17000, with mass discharge rates varying between 0.03 and 0.13 kg/s for the hot fluid and 0.04 to 0.14 kg/s for the cool fluid. The length and diameter of the pipes are 25.4 mm and 2000 mm. The predictive capabilities of the artificial neural network have been used in the modelling of the heat transfer coefficient.

Gorman et al. (2016) endeavoured to investigate the thermal and fluid flow characteristics of a double-pipe heat exchanger featuring a helically corrugated inner pipe wall. A comparative analysis is conducted between a smooth-walled double-pipe heat exchanger and a corrugated double-pipe heat exchanger. The Reynolds numbers observed in the examined cases varied between 420 and 2000.

The experimental and computational analysis of the triple concentric-tube heat exchanger, in comparison to the double tube heat exchanger, was demonstrated by Abdallah Gomaa et al. (2016). The fluid employed in this context is water. The numerical computational fluid dynamics (CFD) model is constructed utilising a finite volume discretization technique and afterwards verified for accuracy and reliability. The paper also includes the presentation of correlations between the Nusselt number, friction factor, and heat exchanger efficacy, with respect to the dimensionless design parameters.

2.5. Heat Exchangers with Nano Fluids

Nano fluid are a unique type of thermal fluid composed of nanometer-sized (less than 100 nm) particles scattered in convectional fluids. This section of the literature review examines the most notable works on Nano fluid technology. Heat transfer enhancement by using Nano fluid is the subject of growing importance in a myriad of applications. So far, there have been few studies related to forced convection. Most of the research is focused on the thermal properties of Nano fluid. Several practical and theoretical research on the increase of heat transfer by Nano fluid are discussed in this literature review. In addition, the influence of nanoparticle concentration, Reynolds number, nanoparticle type, nanoparticle size, and other factors will be examined.

As stated by Senthilraja and Vijayakumar (2013), The heat transfer coefficient of CuO/Water Nano fluid was measured experimentally using a twin pipe heat exchanger. Deionized water with dispersed CuO particles was used to create the Nano fluid. The Nano fluid has   a diameter of 27 nm at ambient temperature and a concentration of between 0.1% and 0.3%. Heat transfer coefficient was shown to increase with time and liquid flow rate was found to enhance the Nusslet number. It was found that the highest heat transfer coefficient was achieved with a 0.3% concentration of Nano fluid.

Sudarmadji et al. (2014), in a double-pipe heat exchanger, researchers examined the heat transfer and pressure drop of an alumina-water Nano fluid. The test section is a 1,1-meter- long, 5-millimeter-diameter inner tube with consistent wall temperatures. The inside of the tube is filled with a hot Nano fluid, whilst the outside is filled with cold

water. The experiment was done with nanoparticle concentrations varying between 0.15 percent, 0.25 percent, and 0.5 percent by volume. The findings demonstrated that an increase in nanoparticle concentration under varying Reynolds numbers causes a rise in convection heat transfer and Nano fluid pressure decrease. Compared to pure water, the Nusselt number increased by 40.5% at a volume concentration of 0.5%, whereas the increase in pressure drop was minimal.

Chavda et al. (2014) examined the effect of using different concentration of Nano fluid on the heat transfer characteristics. A double pipe heat exchanger having Al_2O_3 Nano fluid mixed in water was used in the experiment for parallel flow and counter flow arrangement. The volume concentration of Al_2O_3 Nano fluid was varied from 0.001 % to 0.01 %. The experiment demonstrated that increasing the volume concentration of Al_2O_3 Nano fluid will increase the heat transfer coefficient up to 0.008 % of volume concentration. The coefficient then begins to decline. When comparing water heat transfer in a parallel flow and a counter flow arrangement for a twin pipe heat exchanger, the value of the total heat transfer coefficient increases in the case of Nano fluid of different volume concentrations to water. For parallel flow and at Nano fluid volume concentration of 0.008%, the outer and inner heat transfer coefficient is increased by 101% and 115%, respectively. For counter flow and at the same volume concentration, the increase is 135 % and 136 %.

Firas (2014), in this investigation an experimental and numerical study for U-longitudinal performance with using Nano technology has been performed. The experimental work involved designing and creating four pairs of U-shaped longitudinal fins from copper material, each measuring "1 m in length, 38 mm in height, 1 mm in thickness, 8.2 mm between each pair of U-shaped legs, and 9 mm between each pair of fins". These fins were then welded to a straight copper tube, also 1 m in length, with an inner diameter of 22 mm and an outer diameter of 23.9 mm. Two types of nanoparticles (Al_2O_3 and TiO_2) with (<80, 10-25) nm diameter respectively were dispersed "in de-ionized water". To create Nano fluid, nanoparticle concentrations were (0.2, 0.4, 0.6, and 0.8) percent. At a volume concentration of 0.8 percent, the heat transfer coefficient and thermal conductivity of Alumina-Nano fluid increase by (21 percent, 5 percent) and (16 percent, 4.4 percent) as compared to Titania- Nano fluid. It is obvious that heat transfer enhancement is superior of Alumina-Nano fluid when it is compared with Titania-Nano fluid.

The laminar convective heat transfers of CuO and Cu nanoparticles of sizes 20, 50-60, and 25 nm was tested experimentally by Heris et al. (2006). Water was used as the base fluid, and it was circulated through a circular tube whose walls were kept at a constant temperature. The heat transfer coefficient was determined for varying concentrations of "(Al_2O_3, CuO, Cu)" nanoparticles (from 0.2 to 3.0 percent volume). The experimental findings highlighted the improved heat transfer. This improvement tracked with each Nano fluid's rising volume concentration and Peclet number. The outcomes exceeded those predicted by theoretical correlations. Each Nano fluid has a unique concentration sweet spot where the most improvement can be realized.

Lai et al. (2006) performed an empirical examination on the behaviour of Al_2O_3/water Nano fluid with a particle size of 20nm as it flowed through a stainless steel pipe with a diameter of 1mm. The experiment was conducted under conditions of constant heat flux, specifically at Reynolds numbers below 270. The Nusselt number exhibited an 8 percent rise at a volume concentration of 1 percent.

Ding et al. (2009) Presented numerical simulations of convective heat transfer under laminar flow of TiO_2/water Nano fluid under constant heat flux. Parametric research was conducted on the heat transfer coefficient and wall shear stress for water concentrations ranging from 0 to 10 percent by volume. Both the effect of increasing nanoparticles volume fraction on wall shear stress and the increasing of heat transfer coefficient by 10% with low volume fraction at (Ø ≤ 1.5 %) were obtained.

Experimental research into "Al_2O_3/water and TiO_2/water Nano fluid" was undertaken by Farajollahi et al. (2010) in a shell-and-tube heat exchanger with turbulent flow. Peclet number, particle volume concentration, and particle type were studied for their effects on heat transmission qualities. The results showed that heat conduction was much enhanced when nanoparticles were added to the base fluid. A wide range of volume fractions was employed. The optimal concentration of TiO_2/water Nano fluid has better heat transfer capabilities than the other Nano fluid. Furthermore, as the concentration of nanoparticles in Al_2O_3/water Nano fluid rises, the heat transmission properties of the fluid are enhanced.

Nawaf and Tan (2011) analyzed the performance of a cross-flow heat exchanger using a three- dimensional numerical simulation. Inside a circular pipe, water was picked as the base fluid, while air was chosen for the cross flow. For both sides, numerical simulations were performed using laminar flow. The influence of Reynolds number, Nano fluid type, and Nano fluid volume fraction revealed a considerable increase in heat

transfer with nanoparticles such as "TiO$_2$ nano–powder compared to the base fluid at Reynolds numbers in the range of 500", 1000, 1500, and 2000. In the range of "0.6%, 1.5%, 3%, 6%, and 10%, the volume fraction is between 0.6% and 1.5%". The increase in the Nusselt number was around 6.5 percent for a volume fraction increase of 0.6 to 1.5 percent.

Hydrodynamic and heat transmission properties of 15 nm Al$_2$O$_3$- nanoparticles in laminar flow with continuous heat flux were studied by Esmaeilzadeh et al. (2013). Heat transfer coefficient was shown to rise with increasing particle volume fraction when the effect of varied volume concentrations on the enhancement of heat transfer and friction factor was examined. The results showed that as compared to distilled water, the average heat transfer coefficient rose by 6.8% for a volume concentration of 0.5% and by 19.1% for a concentration of 1%. There was hardly any variation in frictional resistance either.

Using a heat exchanger with and without longitudinal triangular fins, Mathanraj et al. (2018) compared and analysed the heat transfer for counter flow. A 1000mm long, 15mm wide (inside) and 19mm wide (outside) horizontal copper tube serves as the test section. The length, width, and depth of the triangular fin are 8mm, 9mm, and 2mm, respectively. The thermal performance of a heat exchanger is investigated in relation to mass flow rates and fin spacing. The results show that efficiency and heat transfer rate are improved by increasing the mass flow rate of cold fluids. The average logarithmic temperature differential and the total heat transfer coefficient both increase over the course of the experiment.

In order to investigate the impact of geometrical parameters for eight inner corrugated tubes in a double pipe heat exchanger, Córcoles et al. (2020) used numerical analysis. The Realizable k turbulence model of a 3-D unstructured tetrahedral mesh design was analyzed and validated using an experimental result for a turbulence-inducing flow condition (Re=25000). Based on the simulated data, the maximum pressure decreases were observed in the case study with the lowest helical pitch (P/D=0.682) and the highest corrugation height (H/D=0.05). When compared to a flat tube, the maximum number of transfer units is 29% higher.

The influence of inner pipe twisting on the thermal performance of a twin pipe heat exchanger was the subject of an experimental research by Mahmud et al. (2021). The effects of three, five, and seven turns per unit of length in opposite and similar flow directions are studied. All experiments are performed with water as the working fluid in a turbulent flow environment (Re =5000-26000). The experimental results demonstrate

an improvement in thermal efficiency across all three twisted pipes. When compared to a flat pipe, the counter flow increases the Nusselt number by a factor of 2.2, while the parallel flow increases it by a factor of 1.8.

2.6. Summary

Insufficient data exists on the utilisation of Nano fluid for enhancing the efficiency of U-finned tube heat exchangers, despite the fact that many theoretical and experimental studies of Nano fluid are presented to show the effect of concentration, Reynolds number, and type of Nano fluid on heat transfer enhancement. This is what may be deduced from the existing literatures:

1. The heat transfer rate increases with the increasing of Nano fluid concentration.
2. The used of the dual use of nanomaterials with fins leads to a significant increase in the heat transfer coefficient.
3. Many theoretical and experimental researches of Nano fluid are presented to show the effect of concentration, Reynolds number and type of Nano fluid on heat transfer enhancement.

A review of the current literature finds a dearth of knowledge on the topic of employing the Nano fluid technology to improve the efficiency of U-longitudinal finned tube heat exchangers. This study utilizes a 20,4-mm inner diameter and a Reynolds number range of (250) to (2500). Alumina nanoparticles have been employed at volume concentrations 1%, 3%, and 5%. Using a single type of oxide nanoparticles (Al_2O_3), we will numerically model the existing heat exchanger to foretell flow field and heat transfer with and without Nano fluid.

3. MATERIAL AND METHODS

In this chapter, three categories have been discussed as follows: Assumptions are concerned with basic equation heat transfer in double pipe heat exchanger. Thermophysical properties of Nano fluids. Numerical simulation using "ANSYS FLUENT 20" package with "SOLID WORK PREMIUM 2020" to study flow pattern and temperature and velocity distribution in double pipe heat exchanger containing extended surfaces and Nano fluid (Al_2O_3).

3.1. Geometry

Figure 3.1 shows the double pipe heat exchanger. The inner pipe of the heat exchanger has a hot process fluid flowing through it which transfers its heat to the cooling water flowing through the outer pipe. The diameter of the inner tube is (20.4 mm), while the thickness is (1 mm). The diameter of the outer tube is (52 mm), and the total length of the heat exchanger is (1500 mm). Cold water flows inside the outer tube, while the outer surface of the inner tube contains longitudinal U-fin.
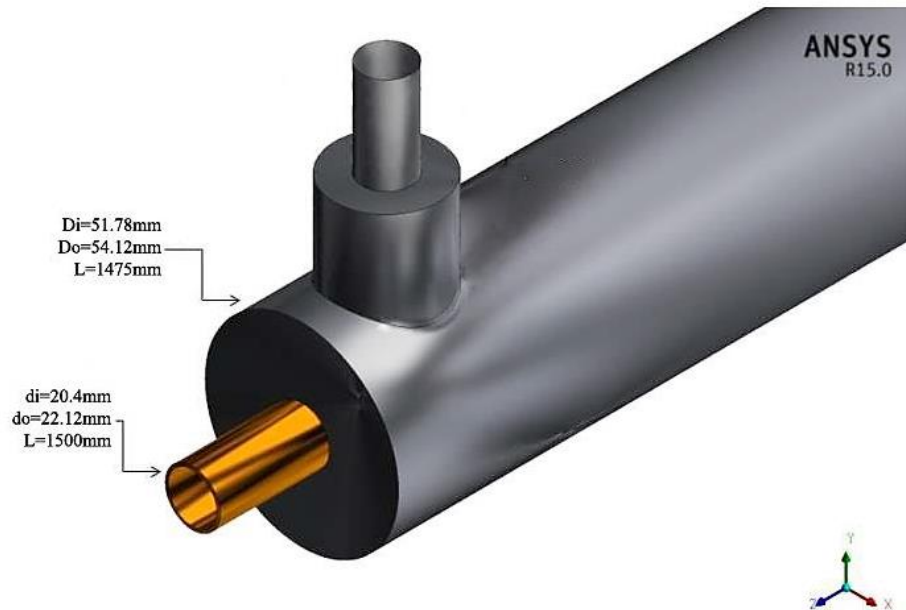
Figure 3.1. Double pipe heat exchanger (all dimensions in mm)

The geometry of a twin pipe heat exchanger and an enlarged surface with inlet and outlet portions for tubes containing hot and cold water are drawn in "SOLID WORK PREMIUM 2020." We insulate the outside pipe of the Annulus.
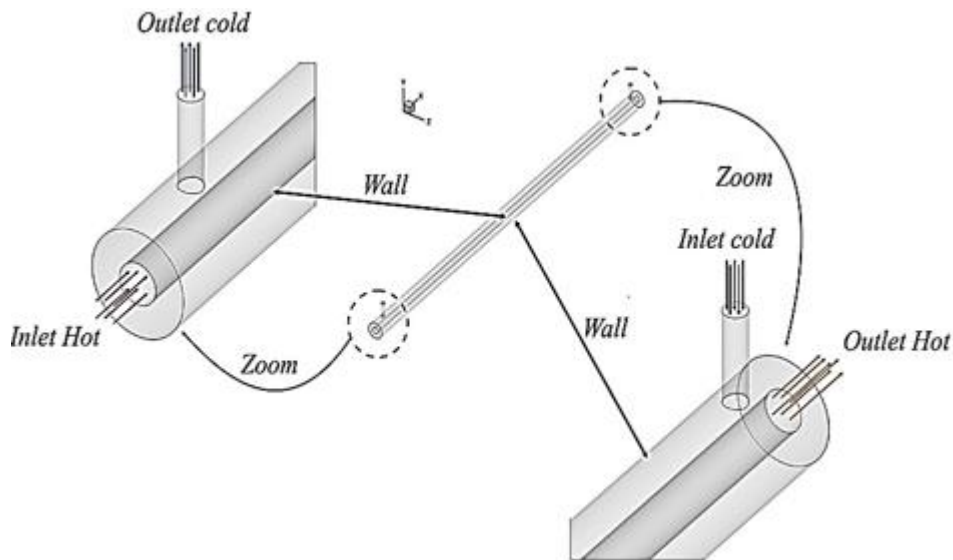
Figure 3.2. The hot and cold fluid temperature distributions in the heat exchanger

Computational domains are depicted as the entry and exit points for the hot water side (inner tube) and the cold water side (annuli) in the current study. As can be seen in Figure 3.3, fins are built onto the outer surface of the inner tube, and the flow on both sides is counter.
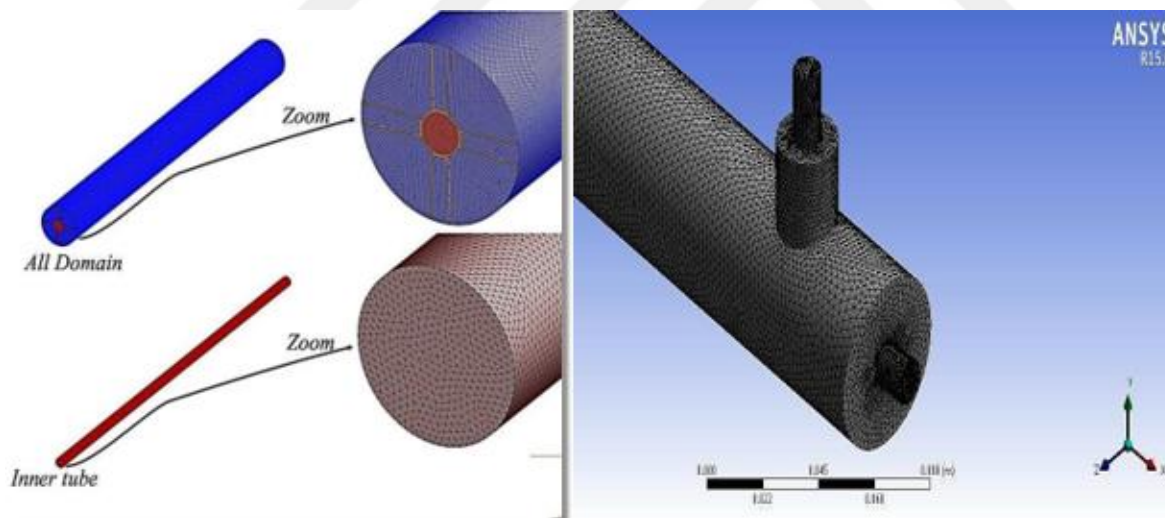
Figure 3.3 The computational domain

3.2. Governing Equations and Data Reduction

For laminar flow in a tube and turbulent flow in annuli, Lars (2015) describes the "governing equations for "Continuity," "Momentum," and "Energy " in the preceding sections.

- Laminar flow

The following governing equations must be solved for laminar flow in an inner tube.

Continuity Equation:

$$\frac{\partial u}{\partial x} + \frac{\partial v}{\partial x} + \frac{\partial w}{\partial x} = 0 \qquad (3.1)$$

Momentum Equation:

$$\rho \left(u\frac{\partial u}{\partial x} + v\frac{\partial u}{\partial y} + w\frac{\partial u}{\partial z} \right) = -\frac{dp}{dx} + \mu \left(\frac{\partial^2 u}{\partial x^2} + \frac{\partial^2 u}{\partial y^2} + \frac{\partial^2 u}{\partial z^2} \right) \qquad (3.2)$$

$$\rho \left(u\frac{\partial v}{\partial x} + v\frac{\partial v}{\partial y} + w\frac{\partial v}{\partial z} \right) = -\frac{dp}{dy} + \mu \left(\frac{\partial^2 v}{\partial x^2} + \frac{\partial^2 v}{\partial y^2} + \frac{\partial^2 v}{\partial z^2} \right) \qquad (3.3)$$

$$\rho \left(u\frac{\partial u}{\partial x} + v\frac{\partial u}{\partial y} + w\frac{\partial u}{\partial z} \right) = -\frac{dp}{dx} + \mu \left(\frac{\partial^2 u}{\partial x^2} + \frac{\partial^2 u}{\partial y^2} + \frac{\partial^2 u}{\partial z^2} \right) \qquad (3.4)$$

Energy Equation:

$$\rho\, Cp \left(u\frac{\partial T}{\partial x} + v\frac{\partial T}{\partial y} + w\frac{\partial T}{\partial z} \right) = k \left(\frac{\partial^2 T}{\partial x^2} + \frac{\partial^2 T}{\partial y^2} + \frac{\partial^2 T}{\partial z^2} \right) \qquad (3.5)$$

-Turbulent flow

The governing equations (continuity, momentum, energy, and transport equations) for turbulent flow in the annuli. In order to obtain answers, it is necessary to solve equations representing various laminar flow types. User's Reference for ANSYS Fluent (2011).

The Data reduction steps are:

- Heat Transfer

The data reduction Eiamsa-ard et al. (2006) of the measured results is summarized as follows also.

Heat transferred to the cold water in the test section, can be calculate:

$$Q_c = \dot{m}_c\, Cp_c\, (T_{c2} - T_{c1} \qquad (3.6)$$

Where, $\dot{m}_c$ is the mass flow rate of the cold water (kg/sec). Cp_c is the specific heat of the cold water (J/kg. K). T_{c2} is the cold water outlet temperature (°C). T_{c1} is the cold water inlet temperature (°C).

Calculate the heat transmitted from the hot water in the test section:

$$Q_h = \dot{m}_h \, Cp_h \, (T_{h2} - T_{h1} \tag{3.7}$$

Where, $\dot{m}$ h is the mass flow rate of the hot water (kg/sec). Cp_h is the specific heat of the hot water (J/kg. K). T_{h2} is the hot water outlet temperature (°C). T_{h1} is the hot water inlet temperature (°C).

The percentage of heat loss Tijing et al. (2006) between the hot and cold-water sides of the current heat exchanger, the following may be stated:

$$\varepsilon = \left(\frac{Q_h - Q_c}{Q_c} \right) * 100\% \tag{3.8}$$

The temperature loss from the test portion to the environment is somewhat low.

For the purpose of calculating the internal convective heat transfer coefficient, the average transfer rate for hot and cold fluids is used.

$$Q_{avg} = \left(\frac{Q_h + Q_c}{2} \right) \tag{3.9}$$

Where, Q_c is the heat transferred to the cold water in the test section (W). Q_h is the heat transferred from the hot water in the test section (W). The surface area of the inner tube is calculated using the following equation:

$$A_i = \pi \, d_i \, L \tag{3.10}$$

Where, di is the inner diameter of tube (m). L is the length of test section (m).

Logarithmic mean temperature difference can be calculated:

$$\Delta T_{lm} = \frac{(T_{h1} - T_{c2}) - (T_{h2} - T_{c1})}{\ln \left(\frac{(T_{h1} - T_{c2})}{(T_{h2} - T_{c1})} \right)} \tag{3.11}$$

The overall heat transfer coefficient is calculated using:

$$U = \frac{Q_{avg}}{A_i \, \Delta T_{lm}} \tag{3.12}$$

Where, Q_{avg} is the average heat transfer rate (W). A_i is the surface area of the inner tube (m²).

The annulus side heat transfer coefficient annulus side heat transfer coefficient (h_a) is estimated using the correlation of Dittus- Boelter Equation (3-13) (Shankar, 2012):

$$Nu = 0.023 \, Re_a^{0.8} \, Pr_c^{0.3} \tag{3.13}$$

Where, Nu_a is the annulus side Nusselt number. D_h is the hydraulic diameter (m), $D_h = D_i - d_o$. Di is the outer tube inner diameter (m). do is the inner tube outer diameter (m). k_c is thermal conductivity of the cold water (W/m. K).

By ignoring the thermal conduction resistance of the copper tube wall, we may calculate the inner tube side heat transfer coefficient (h_i):

$$\frac{1}{U} = \frac{1}{h_i} + \frac{1}{h_a} \tag{3.14}$$

The inner tube side Nusselt number can be calculate:

$$Nu_i = \frac{h_i \, d_i}{k_h} \tag{3.15}$$

Where, h_i is inner tube side heat transfer coefficient (W/m^2. K). k_h is thermal conductivity of the hot water (W/m. k). d_i the inner tube inner diameter (m).

The Reynolds Number Equation (3-16) is based on the different flow rates at the inlet of the test section:

$$Re_i = \frac{u_h \, d_i}{v_h} \tag{3.16}$$

Where, u_h is the velocity of the hot water at the inner tube (m/sec). v_h is the kinematic viscosity of the hot water (N. sec/m^2). The total bulk mean water temperature determines all of the water's thermo-physical characteristics.

- Friction factor

When a fluid is flowing through a tube at a particular velocity, it offers pressure difference due to frictional resistances between the fluid, the twist and the wall. The friction factor, a quantity used to evaluate frictional resistance, is linked to pressure drop in the test section and may be computed as follows:

$$f = \frac{\Delta P}{\left(\frac{L}{d_i}\right)\left(\frac{\rho\, u^2}{2}\right)_h} \quad (3.17)$$

Where, Δp is the pressure drop over the length $L(N/m^2)$. u is the mean velocity of fluid (m/sec). ρ is the density of fluid (kg/m^3). di is the inner diameter of the tube (m).

- Thermal enhancement factor

The ratio of the tube's convective heat transfer coefficient to that of the plain tube is known as the thermal enhancement factor (η) under constant pumping power. It may be stated as follows:

$$\eta = \left|\frac{h_{tu}\, d_i}{h_p}\right|_{pp} \quad (3.18)$$

Using the correlative equation of the Nusselt number for a plain tube and the respective extended surfaces, the thermal enhancement factor is obtained in the following form:

$$\eta = \left|\frac{h_{tu}\, d_i}{h_p}\right|_{pp} = a\, Re^b\, Pr^{0.34} \quad (3.19)$$

3.3. Thermo-Physical Properties of Nano Fluid

The most important formulas and correlations for both volume concentration and physical properties of Nano fluids will be reviewed. Thermal conductivity, viscosity, density and specific heat will be included in the following sections:

3.3.1. Density

The following formula is used to determine the density of Nano fluids:

$$\rho_{nf} = \left(\frac{m}{V}\right) = (1 - \emptyset)\, \rho_{bf} + \emptyset\, \rho_p \quad (3.20)$$

3.3.2. Specific heat

The following mixing rule, which was suggested by Rostamzadeh et al. (2014), is used to calculate specific heat:

$$Cp_{nf} = (1 - \emptyset)\, (Cp)_{bf} + \emptyset\, (Cp)_p \quad (3.21)$$

3.3.3. Volume concentration

The calculation of volume concentration for nanoparticles in base fluid is performed by following relation:

$$\emptyset\% = \frac{\left(\dfrac{m_p}{p_p}\right)}{\left(\dfrac{m_p}{\rho_p}\right) + \left(\dfrac{m_{bf}}{\rho_{bf}}\right)} \tag{3.22}$$

3.3.4. Thermal conductivity

Said et al. (2013) Maxwell and Garnett model is presented as follows:

$$\frac{k_{nf}}{k_{bf}} = \frac{(1 - \emptyset)\left(k_p + 2k_{bf}\right) + 3\varphi k_p}{(1 - \emptyset)\left(k_p + 2k_{bf}\right) + 3\varphi k_{bf}} \tag{3.23}$$

Rostamzadeh et al. (2014) Hamilton and Crossed model is one of the basic formulas which are used as follows:

$$\frac{k_{nf}}{k_{bf}} = \frac{k_p + (n - 1)k_{bf} - \varphi(n - 1)\left(k_{bf} - k_p\right)}{k_p + (n - 1)k_{bf} + \varphi\left(k_{bf} - k_p\right)} \tag{3.24}$$

Where: n = $\frac{3}{\psi}$

In this formula, n is called particle shape factor while ψ is the sphericity which is defined as the ratio of the surface area of a sphere with a volume equal to that of the particle to the surface area of the particle.

$\psi = 1$ is suitable for spherical particles and $\psi = 0.5$ for cylindrical one.

Wasp et al. (1977) simplified H-C correlation for spherical particles by assuming $\psi = 1$, it will be used to calculate the thermal conductivity.

$$\frac{k_{nf}}{k_{bf}} = \frac{k_p + 2k_{bf} - 2\varphi\left(k_{bf} - k_p\right)}{k_p + 2k_{bf} + \varphi\left(k_{bf} - k_p\right)} \tag{3.25}$$

The formula developed by Rostamzadeh et al. (2014) will be utilized in this investigation to determine thermal conductivity.

3.3.5. Viscosity

Einstein has developed a viscosity correlation Said et al. (2013) given by Equation (3.26) in terms of nanoparticle volume concentration in the base fluid, when the nanoparticle volume concentration is lower than 5%, and is given by:

$$\mu_{nf} = \mu_{bf}(1 + 2.5\emptyset) \qquad (3.26)$$

**Table 3.1.** Properties of Nano fluid with different concentration of Al_2O_3

properties	$\phi = 0\%$	$\phi = 1\%$	$\phi = 2\%$	$\phi = 3\%$	$\phi = 4\%$	$\phi = 5\%$
k_{nf} (W/m.K)	0.600	0.610	0.621	0.631	0.641	0.652
ρ_{nf} (kg/m³)	998.2	1027.02	1055.84	1084.65	1113.47	1142.29
μ_{nf} (Kg/m.s)	0.001002	0.001087	0.001198	0.001332	0.001492	0.001676
$C_{p, nf}$ (J/kg K)	4182	4053.21	3931.45	3816.16	3706.84	3603.03
k_{nf} / k_{bf}	1	1.016	1.035	1.051	1.068	1.086
μ_{nf} / μ_{bf}	1	1.084	1.195	1.329	1.489	1.672

3.4. Assumptions

The basic design of double pipe heat exchanger is as shown in Figure 3.4. It has been discussed in details for inner and annuli sides to show the parameters that effect on its performance according to the following assumptions Sadik & Hongtan (2002), Incropera et al. (2007).

1. Steady state condition.
2. The mass flow rate of each fluid remains constant and the fluid properties remain the same.
3. Changes in the kinetic and potential energy are insignificant.
4. The specific heat may be considered constant with little loss of precision.
5. Axial conduction along the tube is typically negligible.
6. The exterior surface of the heat exchanger is believed to be fully insulated, with no internal heat production.
7. There is no phase transition inside the heat exchanger.
8. Counter flow for both fluids passing on both sides of the heat exchanger.

9. No chemical interaction between nanoparticles and base fluid during Nano fluid synthesis or inside the heat exchanger.
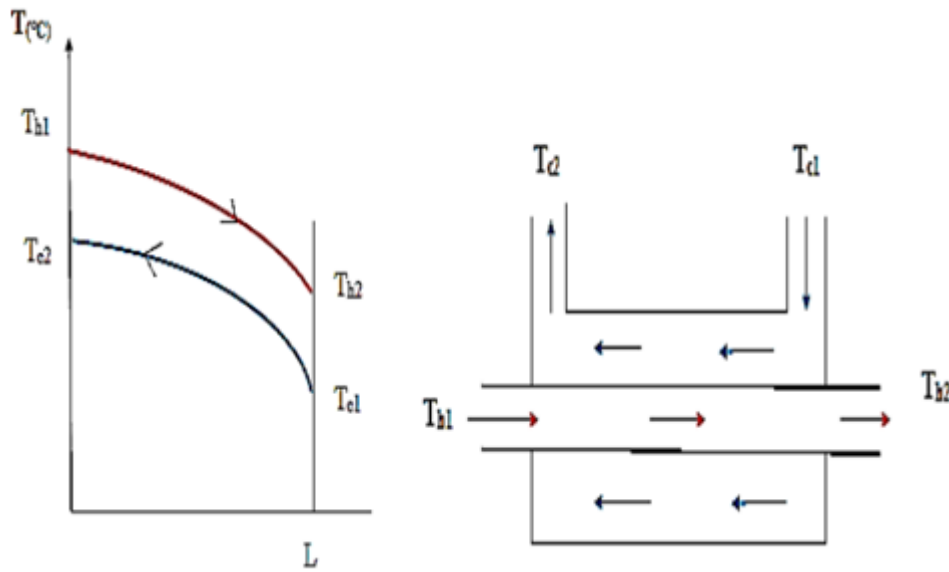
Figure 3.4 The hot and cold fluid direction

3.5. Numerical Simulation Setup and Solving Procedure

Rapid advancements in numerical technique and software, such as CFD codes, have increased engineers' capability to address complex engineering problems. In order to better comprehend the complicated hydrodynamics involved in many industrial processes, CFD algorithms are used to represent the heat and fluid movement. To better understand the intricate fluxes and heat exchange processes occurring within the tube, many researchers have turned to computational fluid dynamics (CFD) modelling. The current research utilized computational fluid dynamics (CFD) modelling with the "FLUENT 20 package" to do numerical simulations on a simulated heat exchanger in three dimensions. The flow field inside the heat exchanger is analyzed using the solutions of continuity, momentum, and energy conservation equations. A smooth, finned tube is tested with and without Nano fluids to see how they affect heat transfer. Subsequent sections will elaborate on the numerical method.

3.5.1. Implementation of boundary conditions

In order to assess the performance of the existing heat exchanger, the following conditions for the physical model must be met:

- Inlet Boundary Conditions:

Velocity inlet was specified various for inner and annuli sides during this study. On the other hand, the temperature inlet of the inner tube is (60°C) while in annuli is (20°C).

- Pressure Outlet Boundary Conditions:

The outlet domain is specified as pressure outlet for both sides.

- Wall Boundary Condition:

No slip boundary condition is specified in the wall of the inner tube. These conditions are used to bound fluid and solid region.

3.5.2. Control parameters

Convenient numerical control and modeling approaches are crucial for enhancing convergence and stability throughout the computation, since they facilitate convergence and stability. FLUENT transforms the governing equations into algebraic equations that may be solved numerically by using the control–volume approach. The control volume method entails integrating the governing equations inside each control volume to get discrete equations. ANSYS Fluent User's Guide (2011).

3.5.3. Computing time and total cell number

In this work, the complexity of geometry that causes acceptable simulation solutions to require a considerable amount of time is identified. When dealing with complex flows, the model's intricate geometry and mesh resolutions may impose limits on the computing time step. In essence, the time step would be constrained by the dense mesh resolution. This study avoids simplifying geometry in order to get the maximum possible degree of accuracy, which may be varied by reducing the resolution as long as the computer's capabilities are adequate to run an accurate simulation. During this experiment, 8.3 million cells are utilized on average.

3.5.4. Number of iterations

It is the maximum number of iterations required to terminate the solution. As seen in the Figure 3.5, (1600) iterations are necessary for this investigation. To avoid divergence solution, the under-relaxation is implemented as follows:

$$\varphi_{new} = (1-\alpha)_{previous} + \alpha\varphi_{calculated} \tag{3.27}$$

Where:

φ_{new}= The new under-relaxed value of φ

$\varphi_{previus}$= The value of φ from the previous iteration.

$\varphi_{calculated}$= The calculating value.

The value for the under-relaxation factor should be in the range of $(0 < \alpha \leq 1)$. The values of α are 0.7 for momentum equation and 0.3 for the pressure. This is because values more than this will cause large instabilities in the solution for laminar and turbulent flow which leads to difficult reaching convergence.
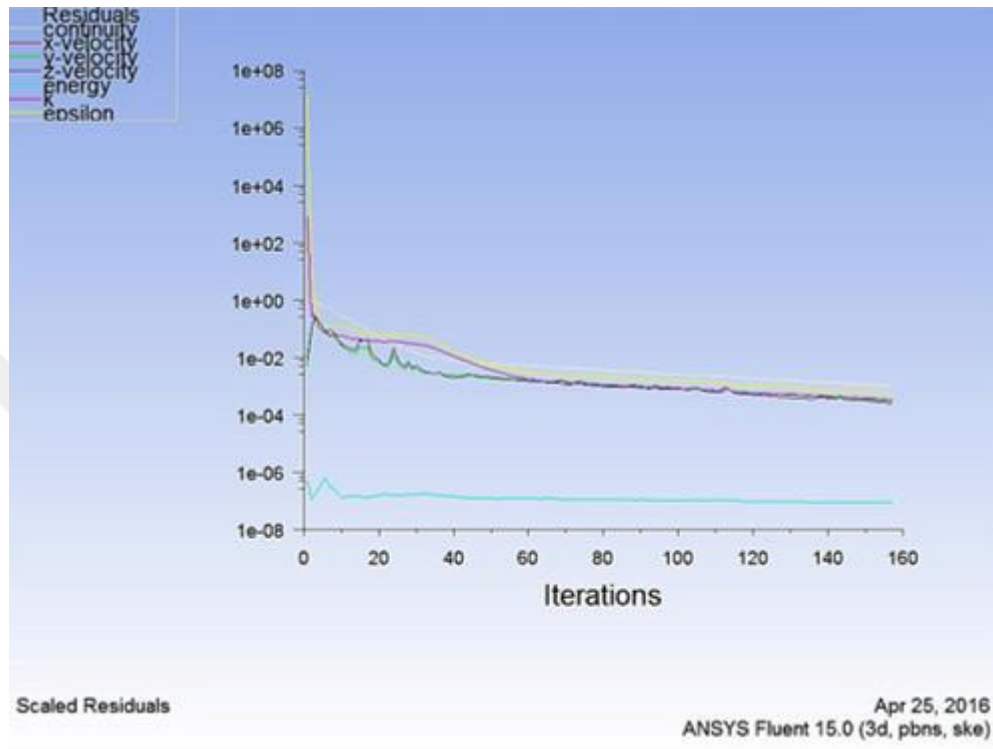
Figure 3.5. Residuals for running of double tube heat exchanger

3.5.5. Convergence

During the iterative solutions of the continuity, velocity, and energy equations for the current investigation, the scaled residual is monitored. For convergence, the following values are considered:

"Residual of <u>continuity</u> = 1×10^{-5}"

"Residual for <u>velocities</u> = 1×10^{-5}"
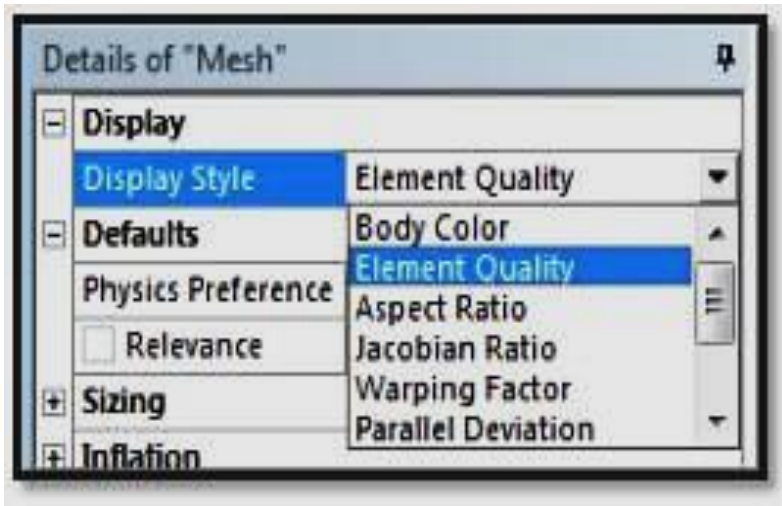
"Residual for <u>energy</u> = 1×10^{-5}"

$K = 1 \times 10^{-5}$

$\varepsilon = 1 \times 10^{-5}$
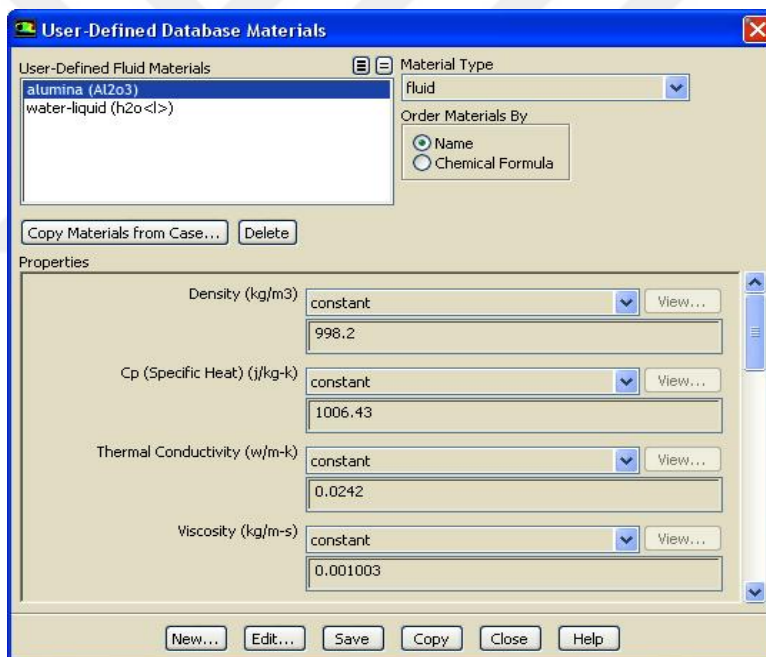
3.5.6. Solving procedure

In FLUENT, the following procedures are carried out in order to accomplish numerical simulation:

1. Examine and read the mesh.

Figure 3.6. Mesh details tool box

2. Determine the model. Standard wall functions are used in the current K– (RNG) simulation model. The energy equation must be enabled.

**Figure 3.7.** User-defined fluid material tool box

3. Discuss the qualities of the following substances: Nano fluids or water (depend on the case) Copper.

4. Present the limiting constraints (section 3.5.7).

5. Select the following for the discretization of differential equations: Pressure = standard Momentum = second order upwind Pressure–velocity coupling = SIMPLE Turbulent kinetic energy = second order upwind

Turbulent dissipation rate = second order upwind

6. Launch the flow field.

7. Calculate using the observation of the scaled residual procedure.
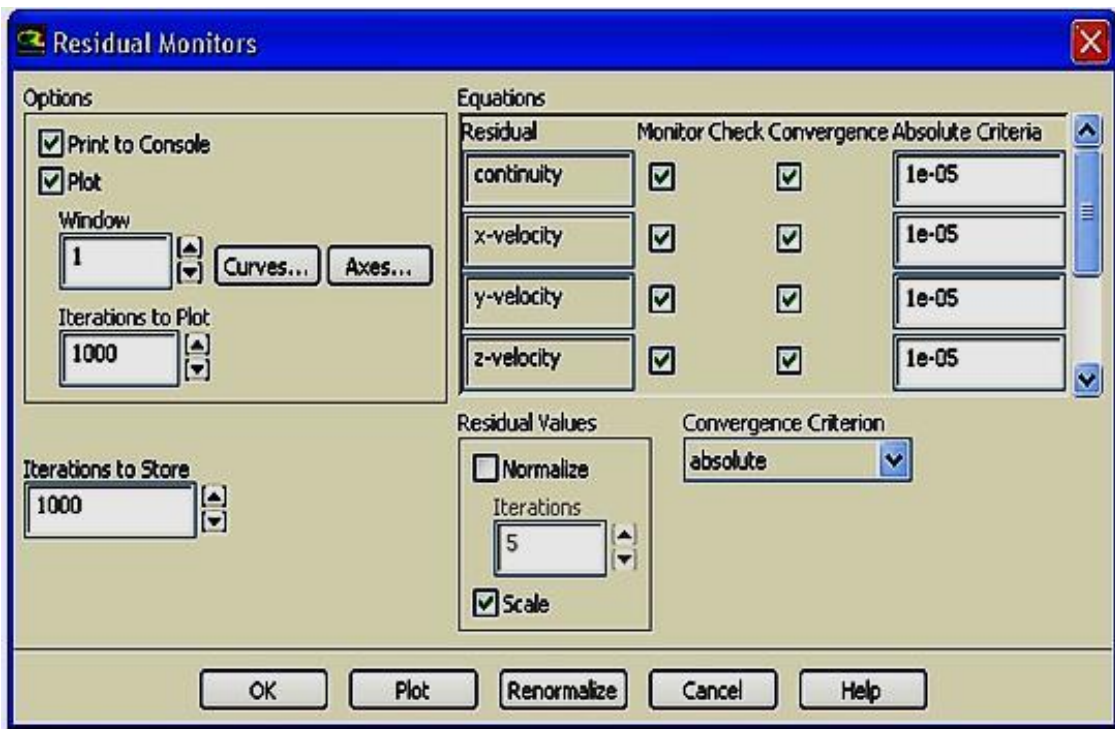
Figure 3.8. Residual monitor tool box

8. Save the findings in the proper folder and convert them to the TECPLOT application in order to display them as described in chapter four.
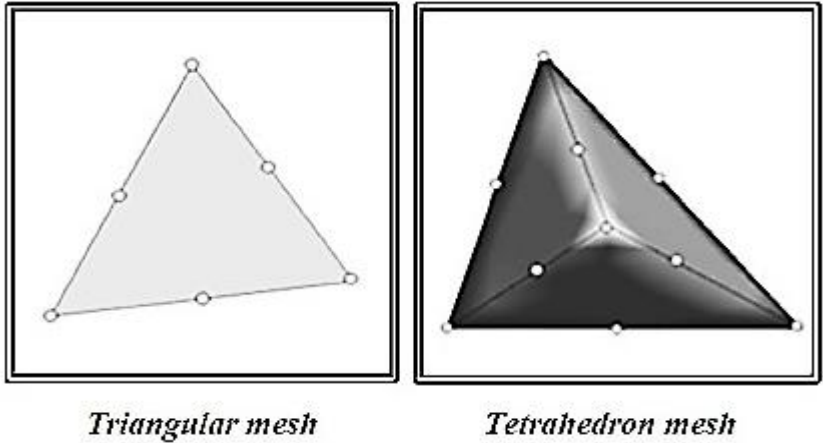
3.6. Mesh Topology

The FLUENT program used an unstructured solver for the unstructured mesh. The arrangement of links changes from point to point in an unstructured mesh. Additionally, the connection of the mesh must be specified clearly using a suitable data structure. Thus, increasing the cost of solution methods compared to structured meshes. However, the higher geometrical flexibility provided by unstructured mesh might be essential when working with domains with complex geometries or when the mesh must be adapted to complex flow field characteristics. In this way, it is possible to apply the superior mesh topology to complex geometries. The FLUENT program supports many element types for mesh topology. Rebay (1993) restricts the number of mesh nodes and the node mode in relation to element forms based on the element type.

This study employs triangular elements for the surface mesh and tetrahedron elements for the three-dimensional geometry. This is due to their precedence in the complex geometries. Figures 3.6 depicts mesh topology.

It is more durable to divide the mesh generation process into subsequent steps including two major issues for further controlling of the mesh. This may have included the followings:

- Surface mesh: It is created for the geometry including the tube surfaces and twisted tape surfaces. A triangular element is used to generate a three-dimensional pave unstructured surface mesh.

- Volume mesh generation: When all surfaces were meshed for each individual area, the volume mesh can now be created for each zone (entrance section and test section) comprising a closed loop of area using T-Grid scheme. Building the mesh requires fine cells in area near tube and twisted tape surfaces, so that it is convenient for turbulent flow characterized. On the other hand, using this element size in the whole domain would lead to an enormous number of elements. That is why it was decided to use a fine mesh in the region near to the surfaces and use coarse meshes as the distance from the surface grows. Therefore, the mesh should be manipulated and controlled manually to keep smooth mesh transition and maintain accurate mesh for a three dimensional model with a minimum computational expense, this has been achieved through the following:

*Triangular mesh*   *Tetrahedron mesh*

Figure 3.9. Mesh topology

4. RESULTS AND DISCUSSION

The numerical results are discussed in great depth in this chapter. Inner tubes with and without fins are studied for their ability to transmit heat. The impact of Al_2O_3 nanoparticles on the thermal conductivity of deionized water is studied. The current heat exchanger with and without fins was simulated numerically in three dimensions using the " $\mathcal{K} - \epsilon$ (RNG) model." Both laminar and turbulent flow can be found on the inner and annuli sides. To evaluate the efficiency of the present heat exchanger, a number of variables are studied numerically. These include the concentration of nanoparticles in volume, the Reynolds number, and the axial distance ratio.

4.1. Mesh Independence Test

The best computing grid can be determined by performing a grid independence test, in which a finer grid yields the same results as the initial grid and the results do not vary as the grid grows finer. Creating a grid with additional cells and comparing the two models' solutions is the approach to determine if the solution is grid independent. Experiments with grid refinement for the Nusselt number show that an approximate grid size of (8) million cells provides sufficient accuracy and resolution to be used as the norm in all circumstances. The results of a grid independence test conducted on a typical heat exchanger with a volume fraction of Ø =3% are depicted in Figure 4.1.
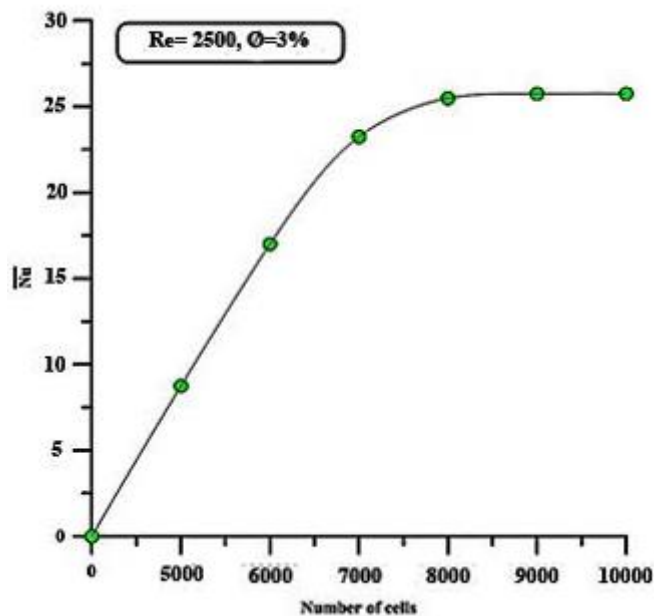
Figure 4.1. The grid independent solution test for typical twisted tape

4.2. Validation of Numerical Results

The results of the present work have been compared to those of the shah equation (Shah, 1975). Nusselt number changes along the inner tube are depicted in Figure 4.2. It should be emphasized that the present work (numerical data) behaves similarly to the shah equation with respect to the hot side.
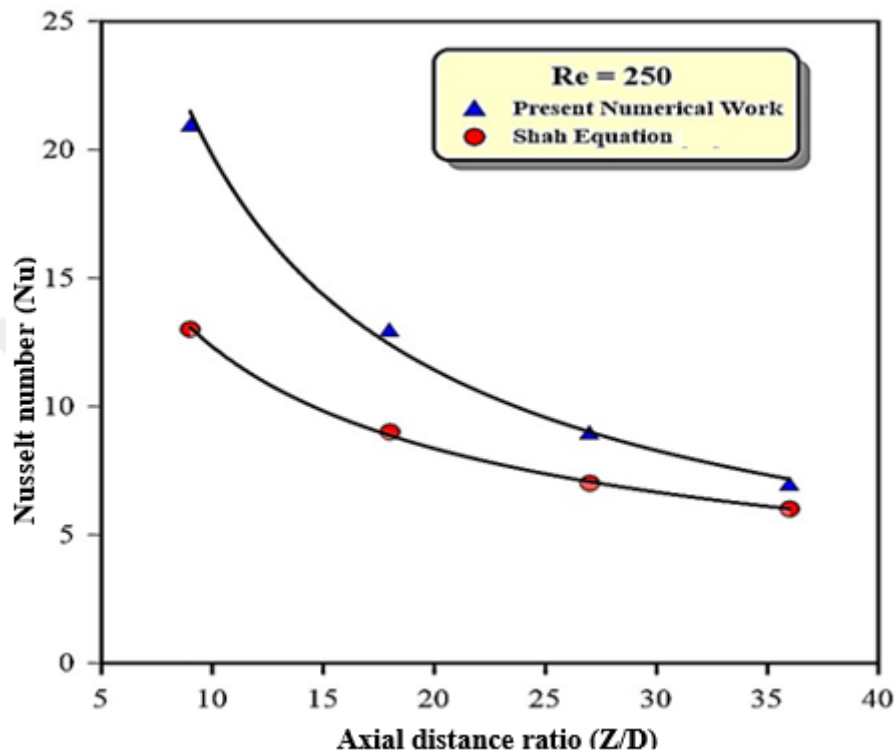

Figure 4.2. Comparison between numerical work and Shah equation

4.3. Heat Exchanger Performance without Nano Fluid

4.3.1. Numerical contours analysis

The existing models' flow field and heat transfer are demonstrated using numerical simulation results generated using ANSYS FLUENT 20. The following sections elaborate on these results:
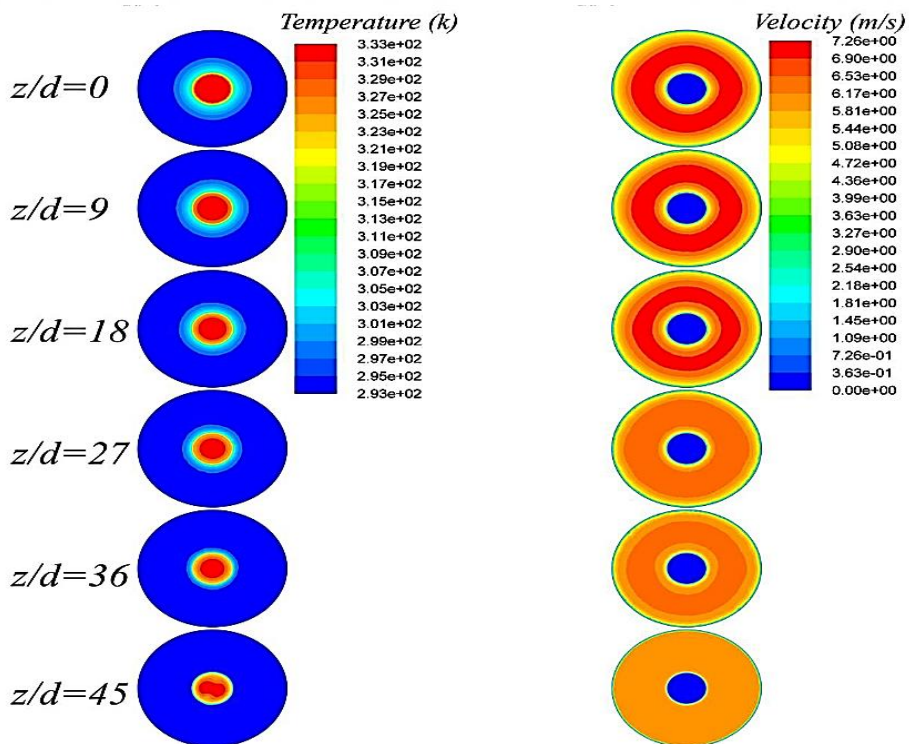
- Temperature and Velocity Contours

The temperature and velocity profiles of a smooth tube heat exchanger at different water Reynolds numbers and axial distances are shown in Figures 4.3, 4.4, and 4.5, respectively. $Z/d = 0$ has the highest cold water temperature and $Z/d = 45$ has the highest hot water temperature. The fact that $Z/d = 18$ indicates that the cold water side will not be significantly affected by a change in the water Reynolds number. It appears that the cold water in annuli is the main source of this phenomena. The figures' velocity contours show that the velocity distribution is constant at the cold water intake at $Z/d = 45$. The

Z/d number dropping from 36 to 0 demonstrates that it will likewise tend to drop inside the heat exchanger, along the inner and outer tube walls.
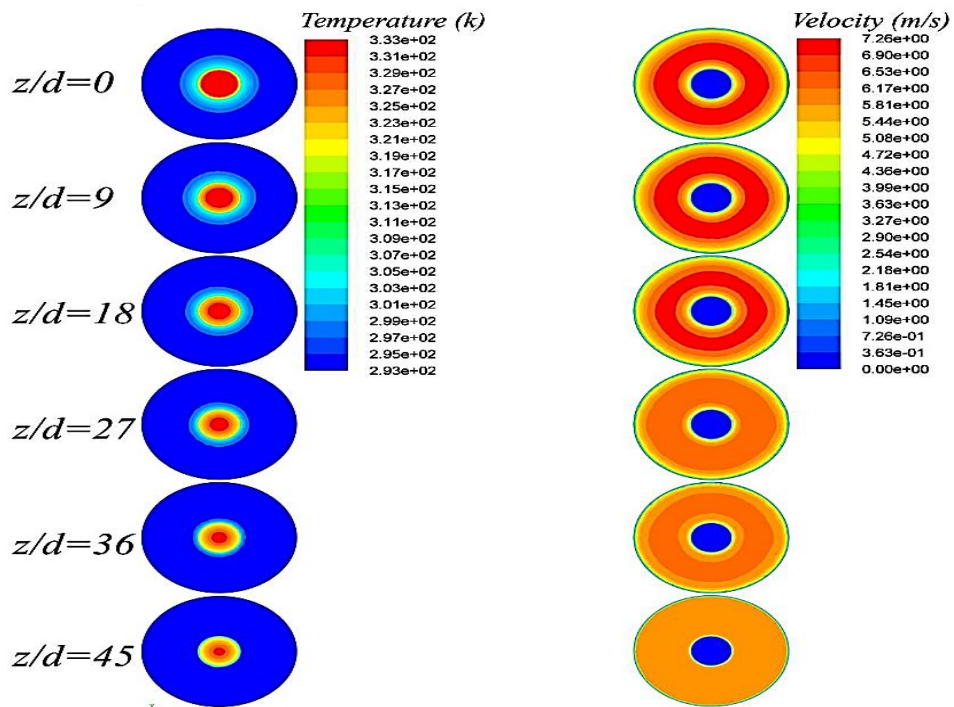
Figure 4.3. Temperature and velocity contours at Re_h=650, and various axial distances for smooth tube heat exchanger

Figure 4.4. Temperature and velocity contours" at Re_h=1400, and various axial distances for smooth tube heat exchanger
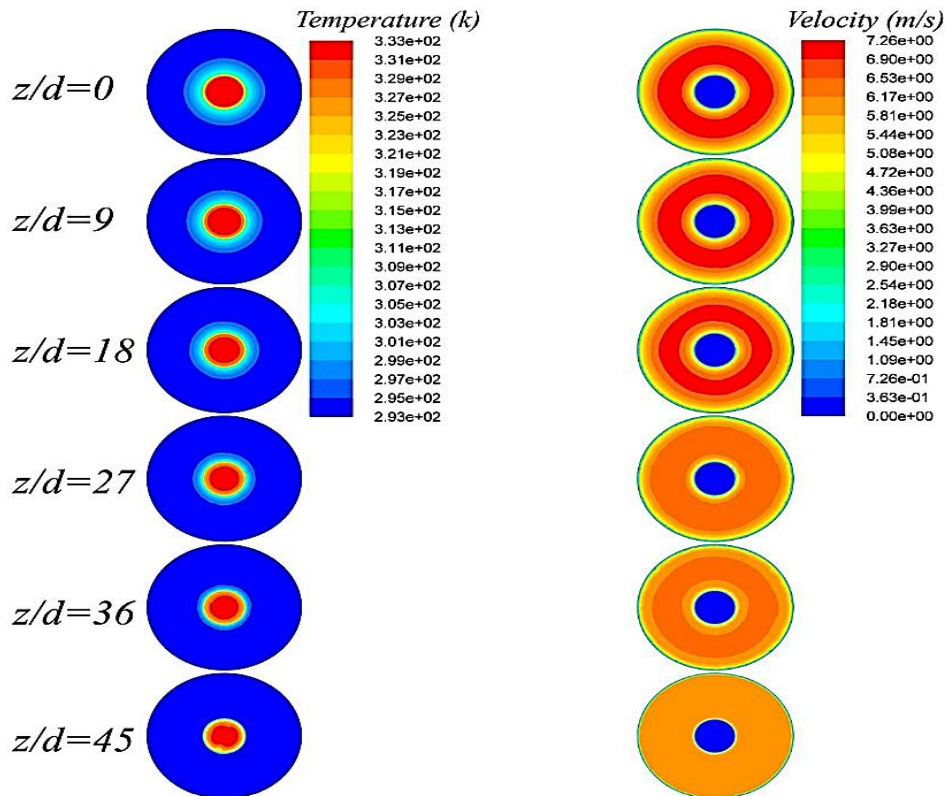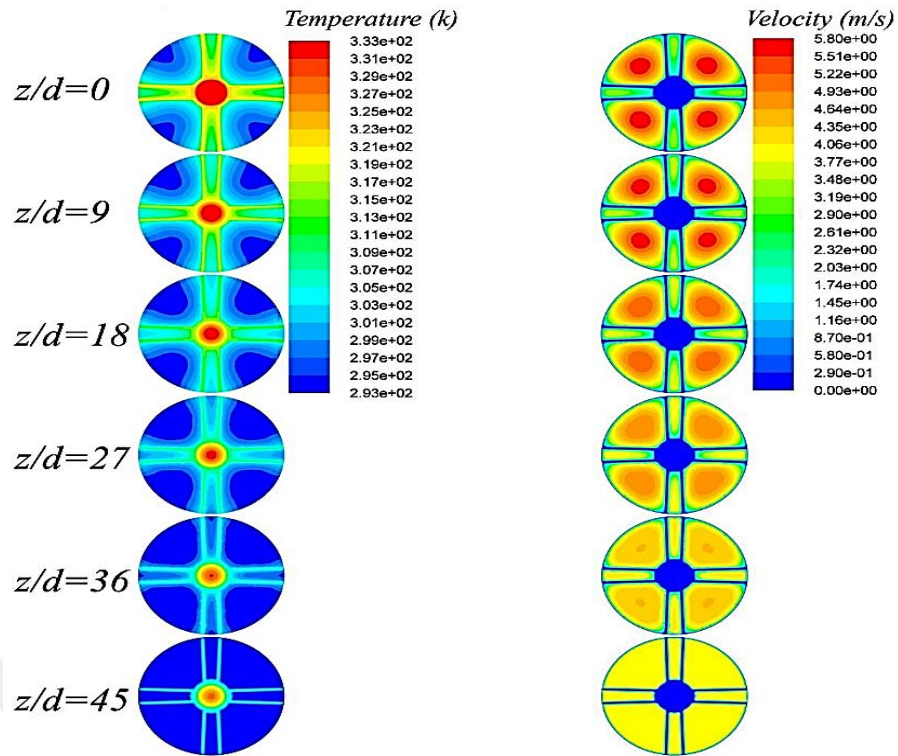
Figure 4.5. Temperature and velocity contours" at Re_h=2000, and various axial distances for smooth tube heat exchanger

Figure 4.6. Figures 4.7, 4.8, and 4.9 depict temperature and velocity profiles of a finned tube heat exchanger for specified hot water Reynolds numbers and cold water mass flow rates at various axial distance ratios. Results revealed a substantial increase in heat transmission for Z/d values between 0 and 45 on both the cold and hot water sides. The effect of fins on thermal transfer is evident from both sides. As the water Reynolds number increases, the behavior of heat transfer enhancement for "Z/d = 27" and " $\dot{m}_c$= 0.025kg/sec" is evident.

As evidenced by the equation "Z/d = 18," it can be observed that an increase in the flow rate to 0.045 kg/sec leads to an augmentation in the temperature difference on the heated water side along the axial distance. Conversely, this increase in flow rate results in a reduction in the temperature difference on the cold water side. The velocity contours presented herein illustrate the consistent velocity of cold water at a dimensionless distance of "Z/d = 45". At the Z/d location, there is a reduction in value from 36 to 0 at the centre between each pair of fins. The graphs clearly demonstrate the impact of the wall on the velocity of both the cold and hot water sides.

Figure 4.6. "Temperature and velocity contours" at Re$_h$=650, and various axial distances for finned tube heat exchanger
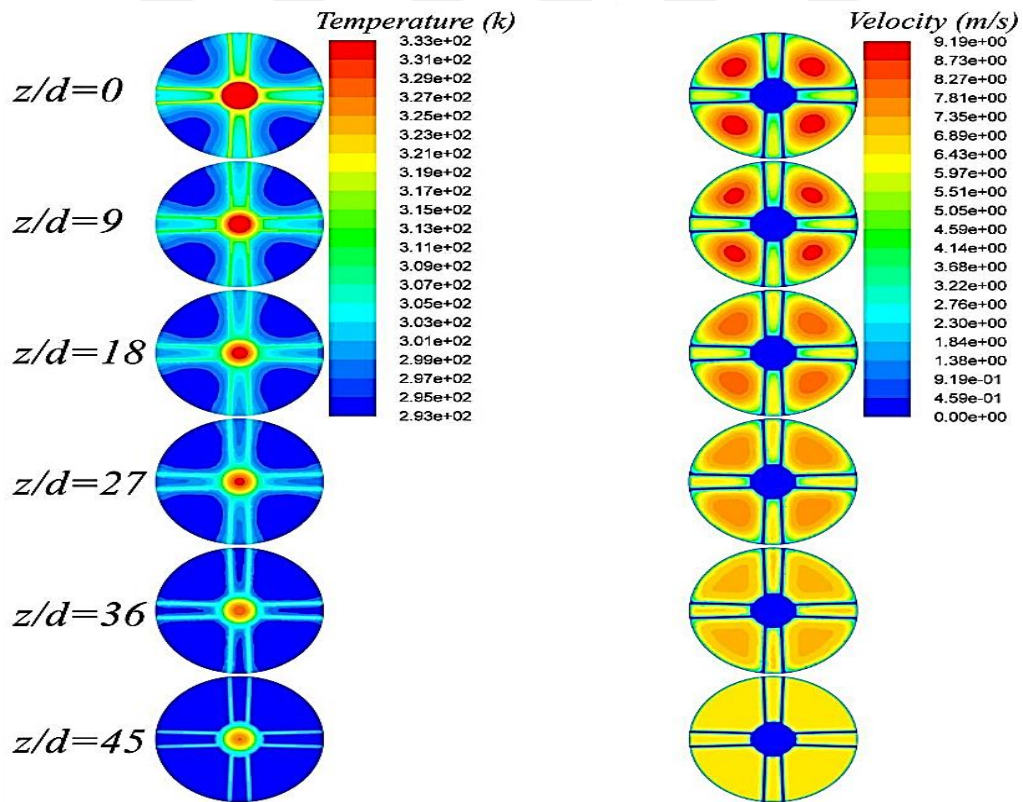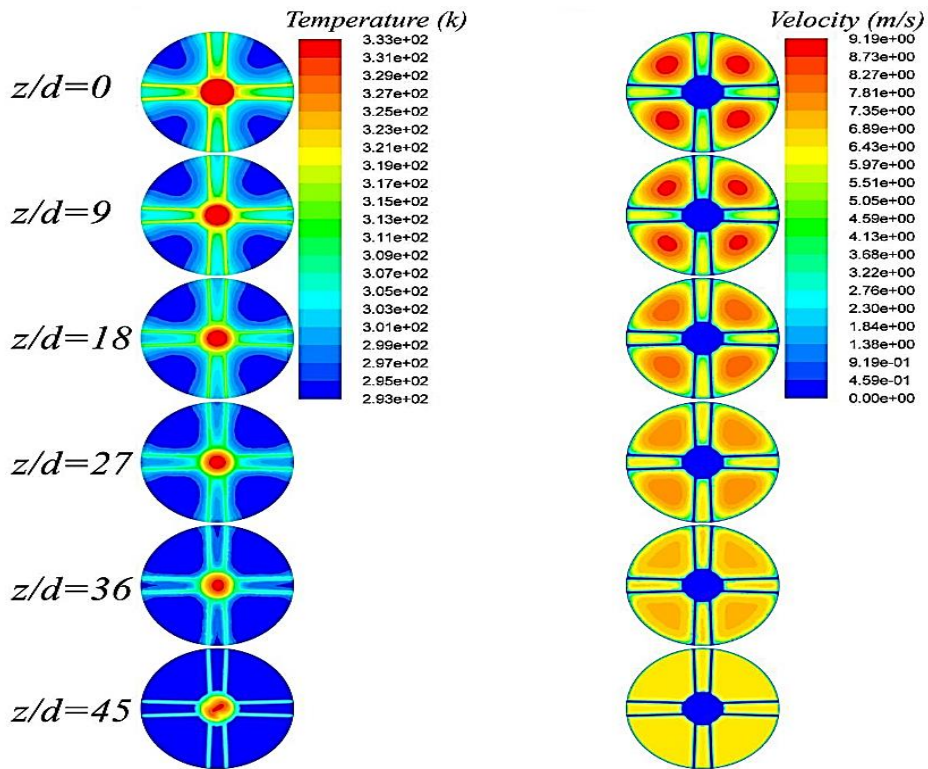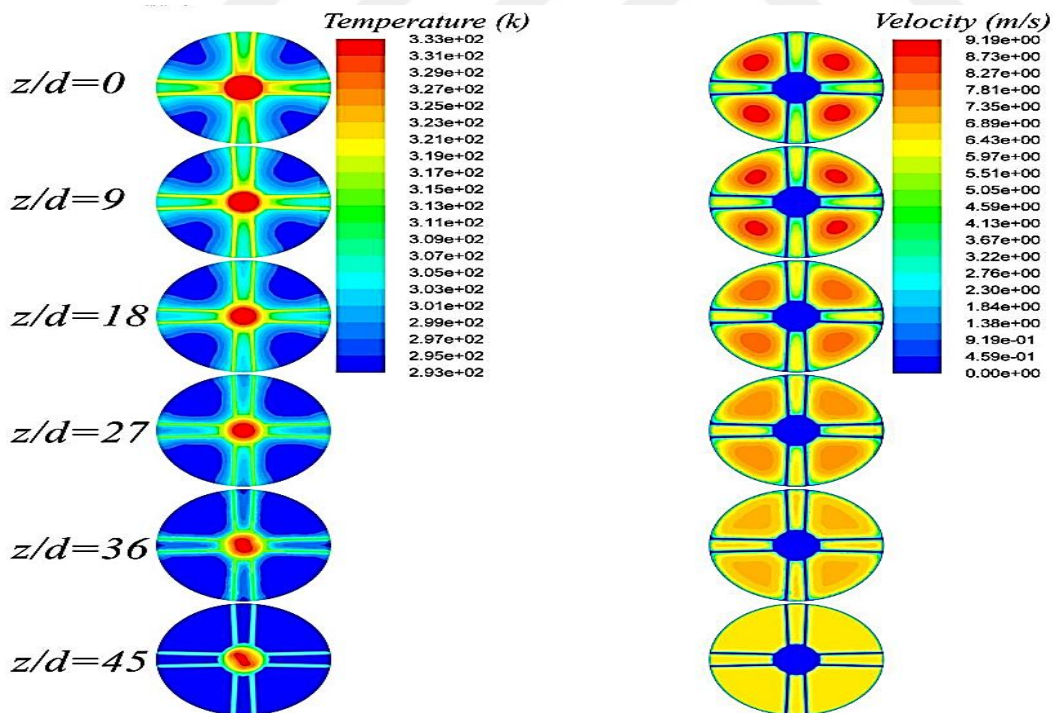

Figure 4.7. "Temperature and velocity contours" at Re$_h$=650, and various axial distances for finned tube heat exchanger

Figure 4.8. Temperature and velocity contours at Re_h=1300, and various axial distances for finned tube heat exchanger


Figure 4.9. Temperature and velocity contours at Re_h=2000, and various axial distances for finned tube heat exchanger

4.3.2. Temperature

Figure 4.10, Figure 4.11, and Figure 4.12 illustrate the relationship between the cold water side temperature differential and the cold water mass flow rate for smooth and finned tube at various hot water Reynolds numbers. As a consequence of the increase in cold water mass flow rate, the cold water temperature differential falls by (57%). The cold water temperature differential on the finned tube is 63 percent greater than on the plain tube. This is a result of the improvement brought about by a larger surface area.
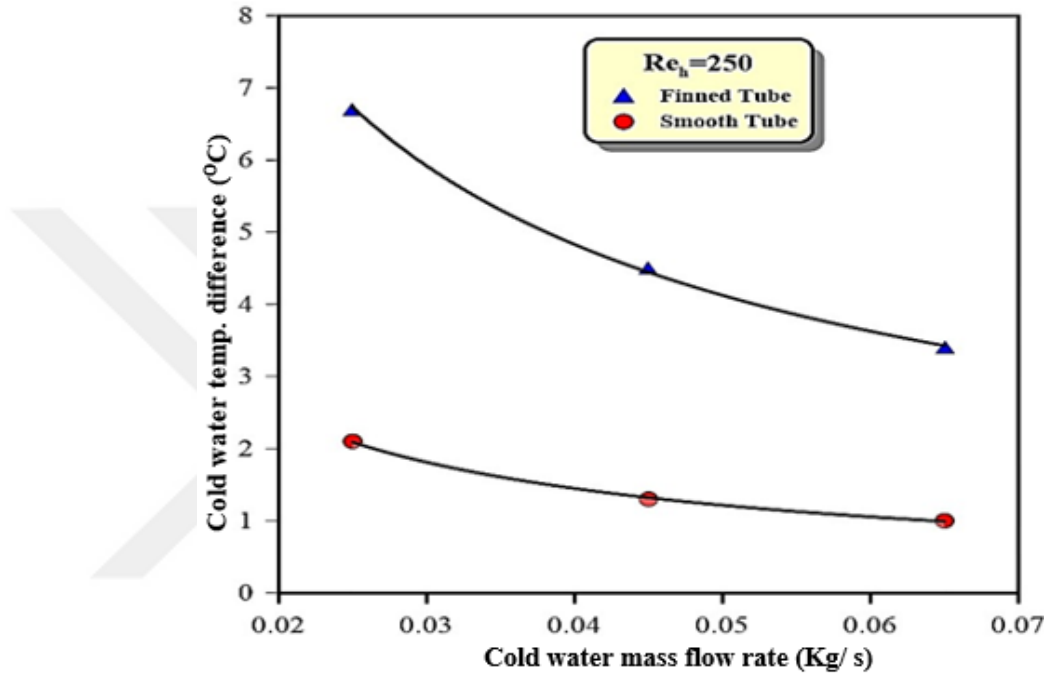
Figure 4.10. Influence of the cold water mass flow rate on the cold water temperature differential at $Re_h = 250$
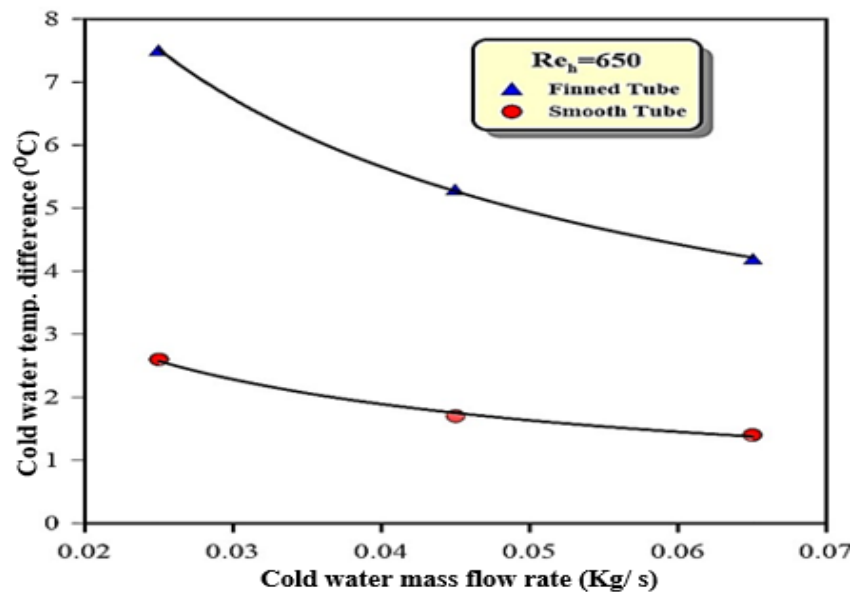
Figure 4.11. Influence of the cold water mass flow rate on the cold water temperature differential at $Re_h = 650$

57
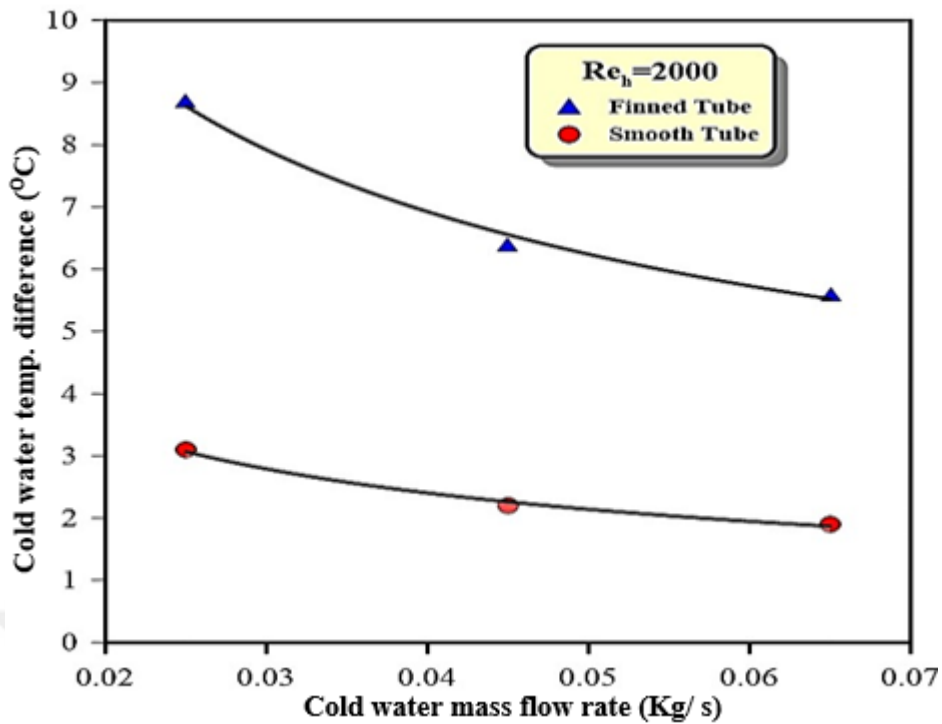
Figure 4.12. Influence of the cold water mass flow rate on the cold water temperature differential at $Re_h=2000$

4.3.3. Heat dissipation

The effect of Reynolds number of hot water on the rate of heat dissipation in smooth and finned tubes are shown in Figures 4.13 and 4.14, respectively. It was performed at numerous values for the mass flow rate of cold water.
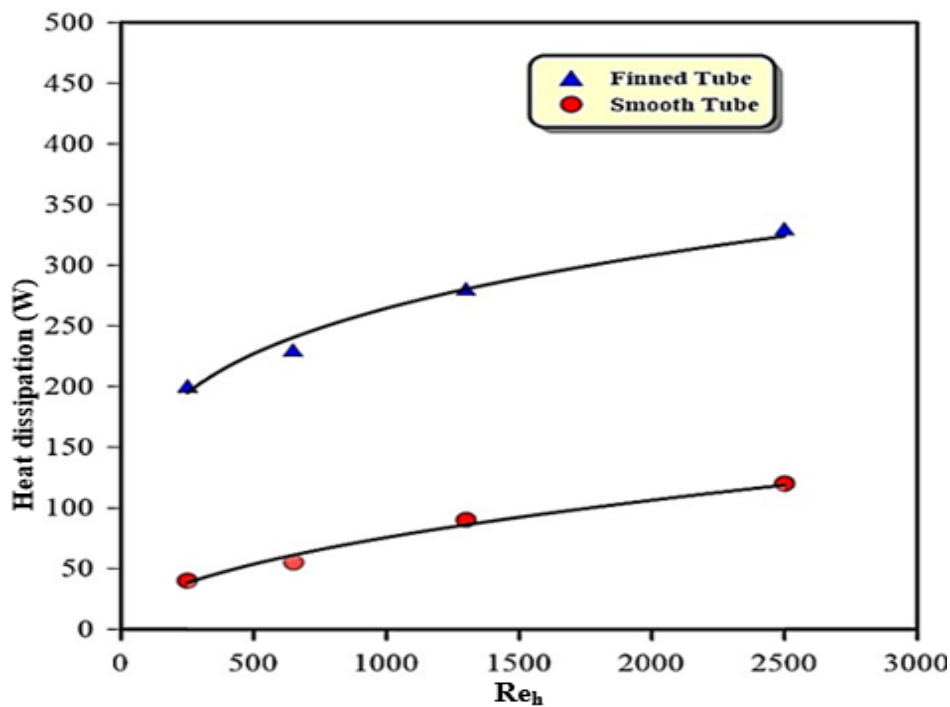
Figure 4.13. Influence of the Reynolds number of hot water on heat dispersion at ṁ=0.025kg/sec

These numbers demonstrate that finned tubes are superior to flat tubes in terms of heat dissipation because of the increased surface area provided by the fins. Heat is dissipated from a finned tube at a rate that is between two and three times that of a smooth tube. Based on these calculations, heat dissipation increases with increasing cold water bulk flow rate.
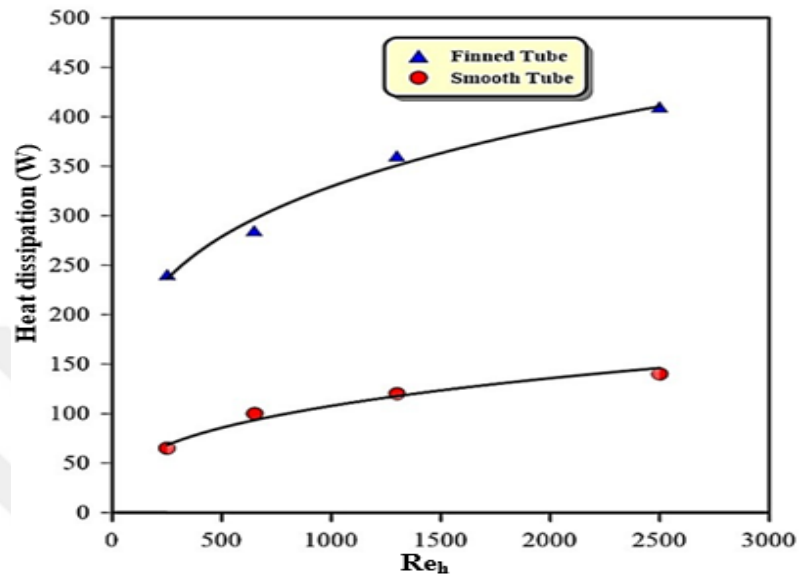
Figure 4.14. Influence of the Reynolds number of hot water on heat dispersion at $\dot{m}$ = 0.045 kg/sec

4.3.4. Heat Transfer Coefficient
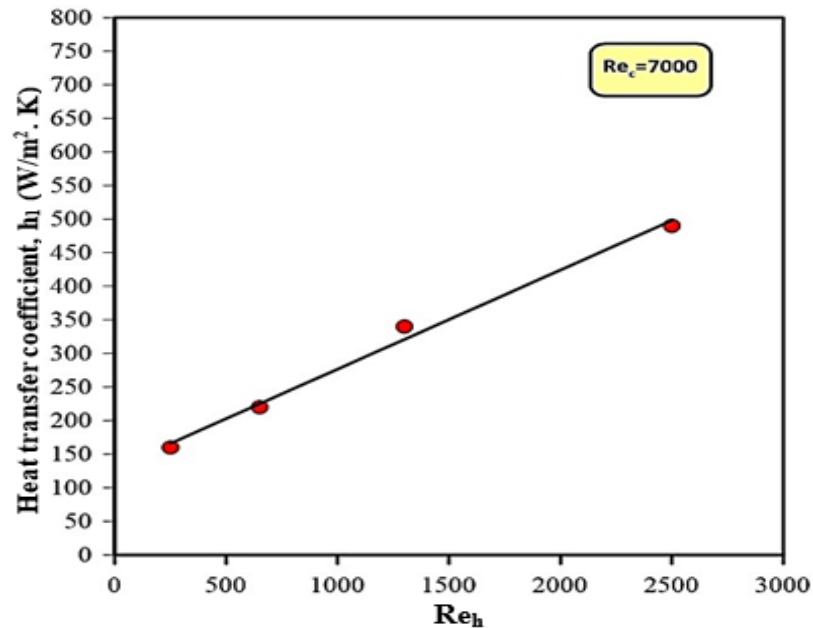
Figure 4.15. Hot water's effect Reynolds number influence on heat transfer coefficient for finned tube at Re_c =7000

In Figure 4.15 and 4.16, we see how changing the Reynolds number of the hot water has an effect on the inner heat transfer coefficient at different Reynolds numbers. It has been demonstrated that an increase in the water's Reynolds number causes turbulence, which in turn increases the heat transfer coefficient on the hot water side. When the cold water Reynolds number is raised, the hot water side's heat transfer coefficient drops by 4%.
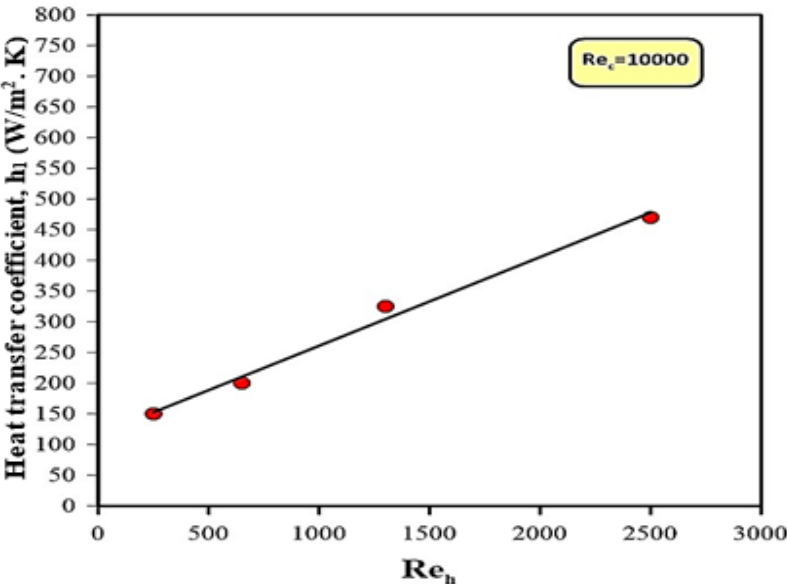
Figure 4.16. Hot water's effect Reynolds number influence on heat transfer coefficient for finned tube at $Re_c = 10000$

As shown in Figure 4.17 and Figure 4.18, for different hot water Reynolds numbers, the annuli heat transfer coefficient varies in relation to the cold-water mass flow rate in both smooth and finned tubes.
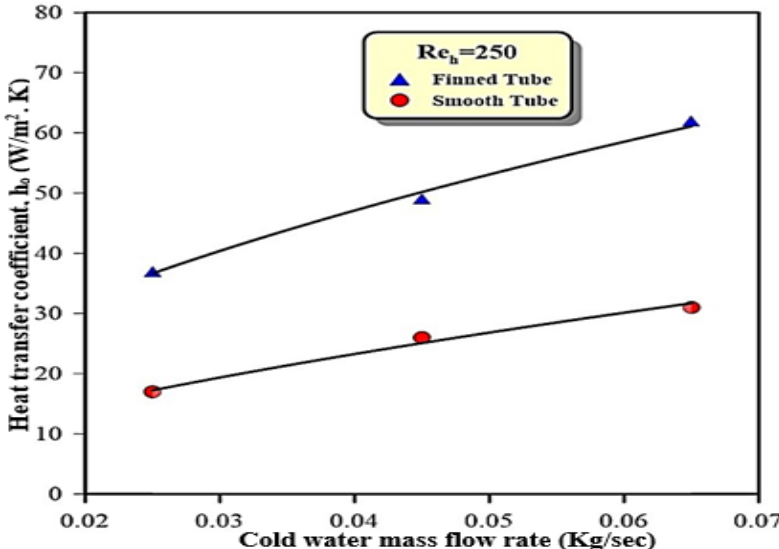
Figure 4.17. The influence of cold water mass flow rates on the cold water heat transfer coefficient at $Re_h=250$

The increase in the cold-water heat transfer coefficient can be attributed to the turbulence that was produced by the higher cold-water velocities. The heat transfer coefficient of finned tubes is greater than that of smooth tubes because of the additional surface area provided by the fins. Based on the results of this study, the amplification factor in the heat transfer coefficient from cold water falls within the range of (1.6 to 2). The annuli heat transfer coefficient decreases by 9% (250-650) when the Reynolds number of hot water is increased from 1 to 2.
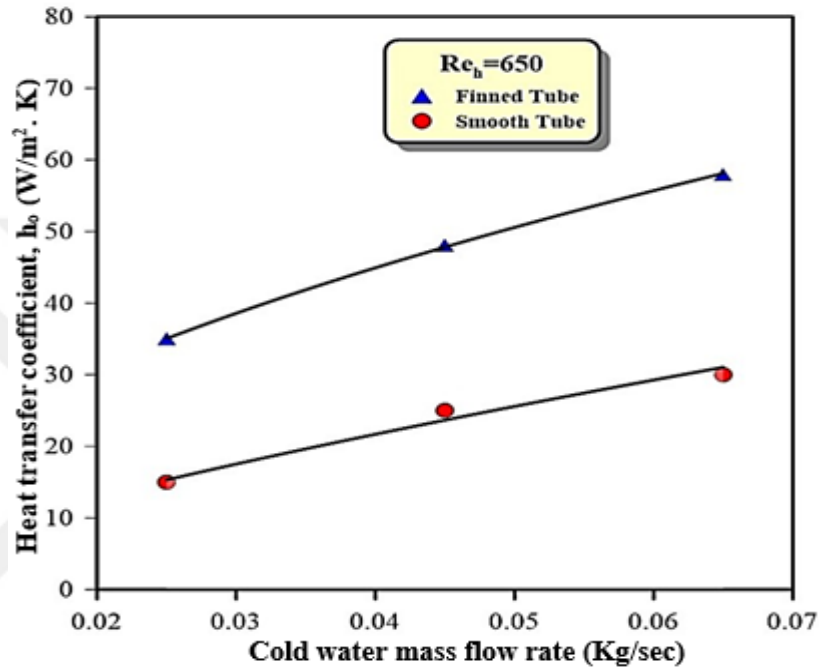
Figure 4.18. The influence of cold water mass flow rates on the cold water heat transfer coefficient at Re_h= 650

4.4. Heat Exchanger Performance with Nano Fluid

Nano fluid performance in finned tube heat exchangers has been studied in relation to nanoparticle concentration in the fluid. When simulating Nano fluids, cold water was given a Reynolds number of 13000. The thermal performance of heat exchangers with Nano fluids is discussed below.

4.4.1. Numerical contours analysis

Figures 4.19, 4.20, and 4.21 depict the temperature and velocity contours of a finned tube heat exchanger utilizing Nano fluids, respectively. Notably, the enhancement of heat transmission on the cold water side occurs for Z/d values between 0 and 18. However, Z/d ranges from 27 to 45 for the hot water side of things. Even though the increase in thermal conductivity is rather modest, the thermos-physical properties of Nano

61

fluid are primarily responsible for this increase. By increasing the thermal conductivity of the basal fluid, this improvement in heat transfer behavior can be augmented further.
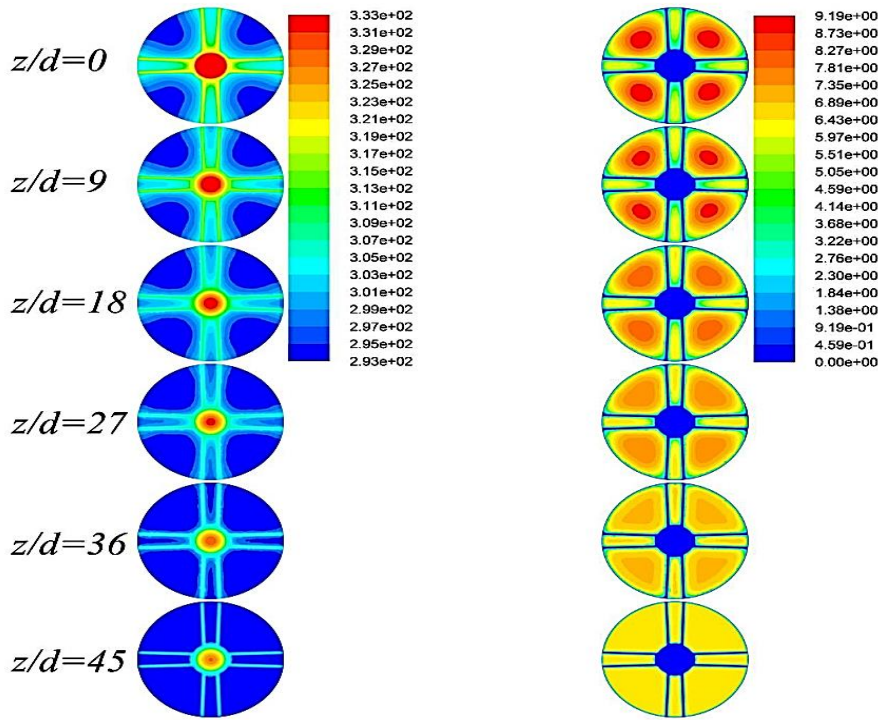
Figure 4.19. Temperature and velocity contours" at Re_h=650, as well as a number of different axial distances for the finned tube heat exchanger using the Alumina-Nano fluid
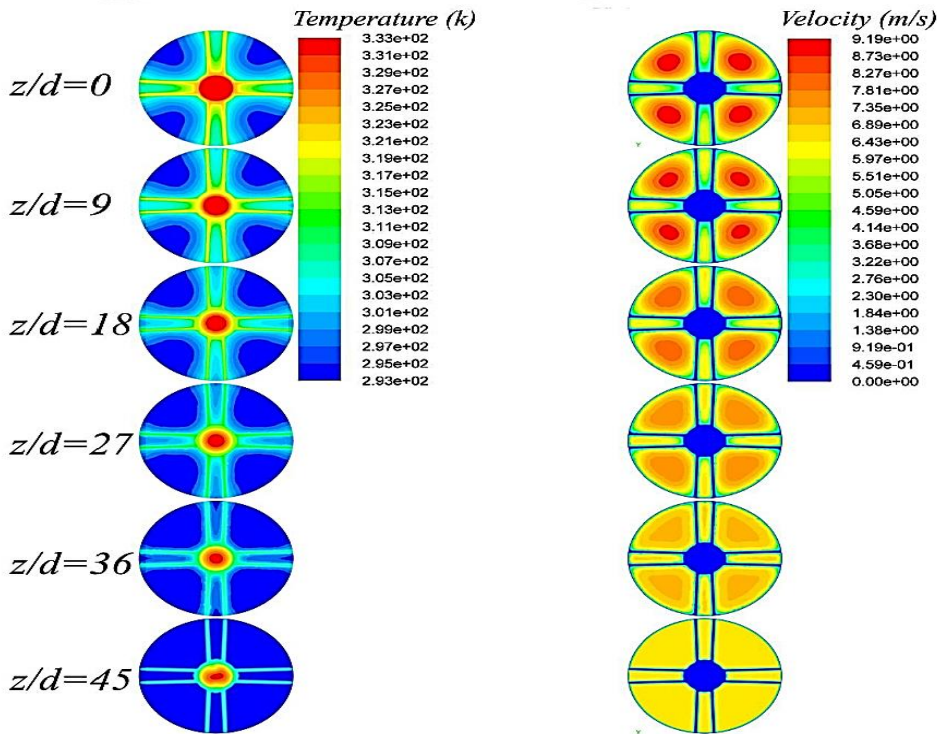
Figure 4.20. Temperature and velocity contours at Re_h=1300, as well as a number of different axial distances for the finned tube heat exchanger using the Alumina-Nano fluid
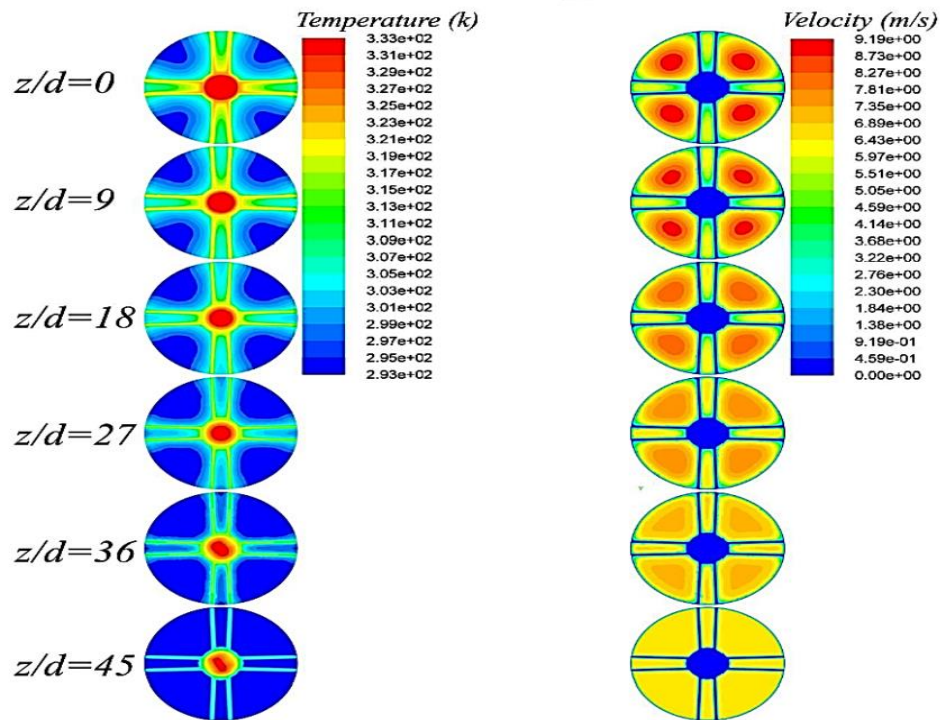
Figure 4.21 Temperature and velocity contours at $Re_h=2000$, as well as a number of different axial distances for the finned tube heat exchanger using the Alumina-Nano fluid

4.4.2. Heat dissipation

The correlation between the Reynolds number and heat dissipation in an Alumina-Nano fluid is shown in Figure 4.22. It is evident that heat dissipation is enhanced with an increase in the concentration and Reynolds number of the Nano fluid. Figure 4.23 displays the volume concentration dependence of the heat dissipation in Alumina-Nano fluids. The enhanced heat dissipation of Alumina- Nano fluids over a base fluid is shown in Table 4.1. The growth was unlimited (18.9 %).

Table 4.1 Enhancement of heat dissipation with Alumina-Nano fluid

Re	Volume Concentration (%)	Qnf/Qbf	Enhancement (%)
250	0%	1	0
250	1%	1.04	3.8
250	3%	1.08	7.4
250	5%	1.2	16.6
650	1%	1.16	14.2
650	3%	1.23	18.9
650	5%	1.3	23.2

Re	Volume Concentration (%)	Qnf/Qbf	Enhancement (%)
1300	1%	1.08	7.6
1300	3%	1.13	12.1
1300	5%	1.19	16.2
2500	1%	1.09	8.6
2500	3%	1.14	12.5
2500	5%	1.22	18.4
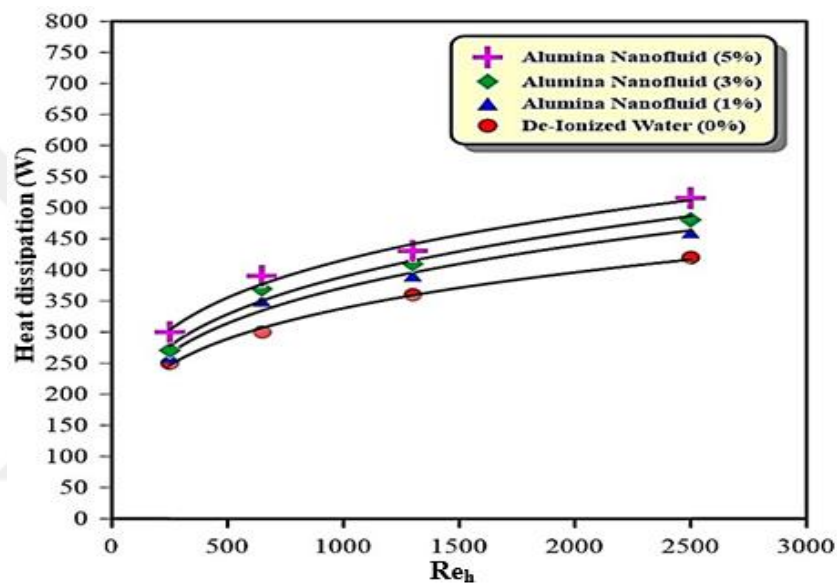
Figure 4.22 The effect of Reynolds number on the heat dissipation of Alumina-Nano fluid at different concentrations of volume
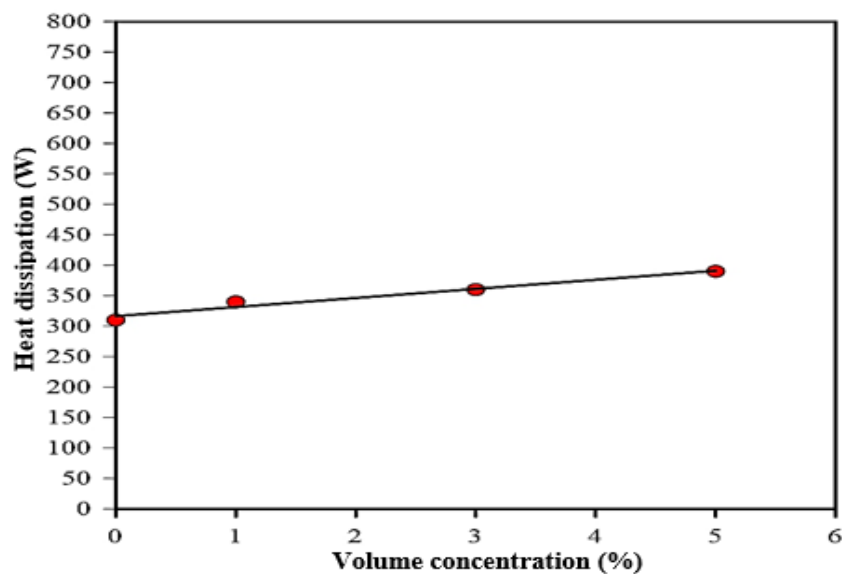
Figure 4.23. Variation in heat dissipation as a function of Alumina-Nano fluid concentration

4.3.3. Heat Transfer Coefficient

The fluctuation of the heat transfer coefficient of Alumina-Nano fluids with varying Reynolds number and nanoparticle volume concentration is shown in Figure 4.24. This graph indicates that the heat transfer coefficient increases as both the Reynolds number of the Nano fluid and the nanoparticle volume concentrations in the base fluid increase.
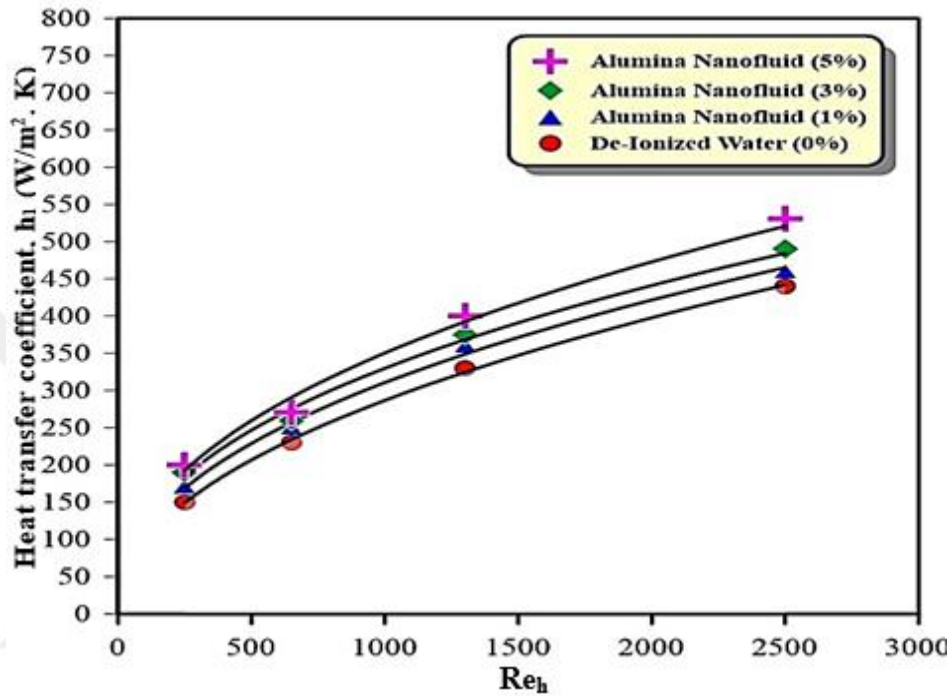
Figure 4.24. Variations in the inner heat transfer coefficient as a function of the inner Reynolds number for Alumina-Nano fluid at varied concentrations
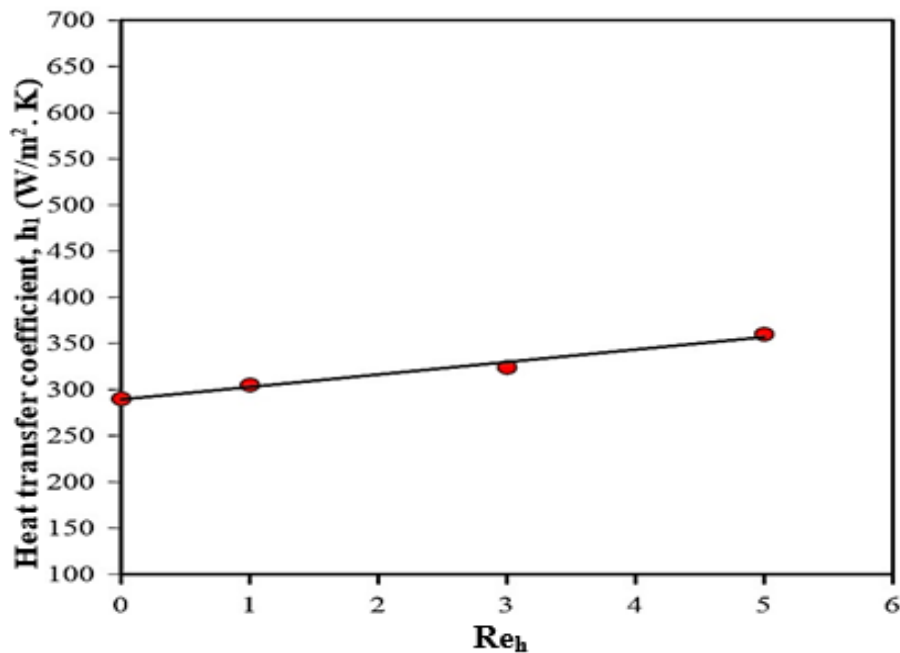
Figure 4.25. Variation of the inner heat transfer coefficient with Alumina-Nano fluid concentrations

Increasing the nanoparticle volume concentration increases thermal conductivity and reduces the thickness of the thermal boundary layer. This is due to the mobility of particles near the wall, their migration to the center of the tube, and the reduction in viscosity near the wall. Figure 4.25 depicts the effect of volume concentration on the heat transfer coefficient in Alumina-Nano fluids.

4.4.4. Heat transfer enhancement (Nu number)

In Figure 4.26, we see the effect of increasing the Reynolds number on the Nusselt number for Alumina-Nano fluids.
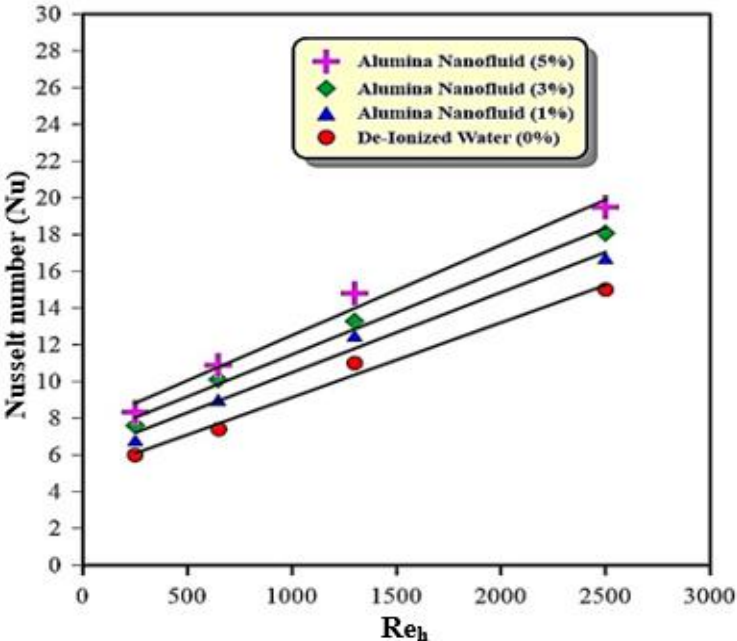
Figure 4.26. Effect of inner Reynolds number on inner Nusselt number for Alumina-Nano fluid at varied volume concentrations
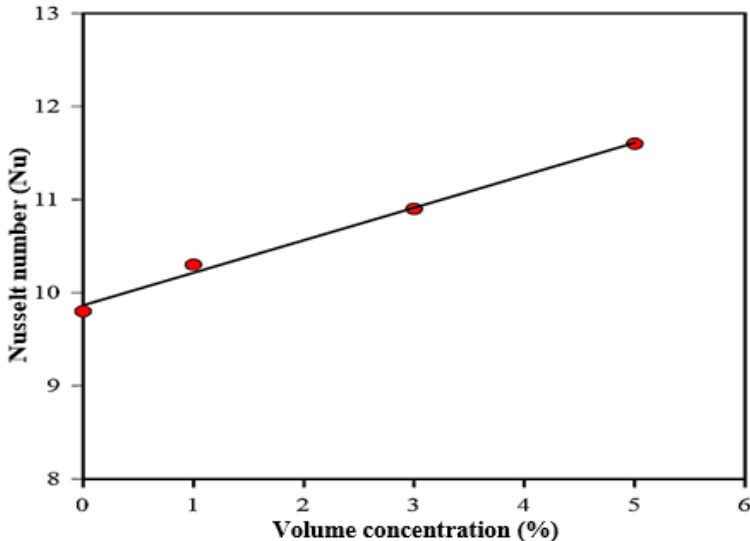
Figure 4.27. Variation of the inner Nusselt number with Alumina-Nano fluid concentrations

These numbers demonstrate that an increase in both the Reynolds number and the nanoparticle volume concentration leads to an increase in the Nusselt number. This enhancement can be attributed mostly to Nano fluid's enhanced thermal conductivity and heat transfer coefficient. Figure 4.27 shows how the Nusselt number changes as a function of concentration in Alumina-Nano fluids.

5. CONCLUSION AND RECOMMENDATIONS

5.1. Conclusions

This paper presents a numerical investigation of the heat transmission in a double-pipe heat exchanger with fins implanted on the outer surface of the inner pipe. The investigation is conducted using a novel technique that incorporates Nano fluid to improve thermal transfer. The primary conclusion of this study can be stated as follow:

- The improvement in heat transmission is seen when fins are added to the outer surface of the inner tube in the current heat exchanger. This improvement is seen in the heat dissipation and cold water heat transfer coefficient values, which are (2.3 to 3.1) and (1.6 to 2) times that of a smooth tube, respectively.

- The temperature difference observed on the hot water side has a direct relationship with the mass flow rate of the cold water, and experiences a reduction of 66% as the Reynolds number of the hot water increases.

- The temperature difference on the cold water side exhibits a direct correlation with the Reynolds number of the hot water and experiences a reduction of 57% as the mass flow rate of the cold water increases.

- The incorporation of nanoparticles into the base fluid significantly enhances the heat transfer coefficient of the existing heat exchanger. According to the findings, the maximum observed increase for alumina nanoparticles is 20% when the volume concentration is set at 5%.

- Adopting fins on the outside surface of the inner tube significantly improved the efficacy of heat exchangers.

- The addition of fins to the heat exchanger enhanced heat dissipation, according to the simulation results. In this model, cold water mass flow rates and hot water Reynolds numbers have increased.

- According to a computer simulation, adding nanoparticles to the base fluid improves heat transmission.

- The results of a numerical simulation demonstrated that adding fins to a heat exchanger would increase heat dissipation. It is observed that heat transfer behavior improves as air mass flow rates and water Reynolds numbers increase within the current model.

5.2. Future Work

The following suggestions are made for further expansion of the current work:

- Studying the effect of adopting other types of base fluids like oil, ethylene glycol and refrigerants.
- Using other types of nanoparticles such as (Fe_2O_3 and CuO) to verify the enhancement in heat transfer compared with (Al_2O_3) that used in present study.
- Studying the effect of adding internal fins on thermal performance of heat exchanger.
- Investigating the performance of other types of extended surfaces (pins, serrated, …etc.) in annuli side.
- Studying the effect of adding twisted tape insert to the inner tube on heat transfer enhancement.
- Studying the effects of changing fin shape on cold water side heat transfer coefficient.
- Studing the effect of shape factor of Nanofluid on the heat transfer rate and augmentation factor

6. REFERENCES

Adrian B. and Allan K. D. (2003). Heat transfer enhancement. In: *Heat Transfer Handbook* (Ch. 14, pp. 1033-1101). Wiley.

Ali, M. H., & Jalal, R. E. (2021, July 30). Experimental investigation of heat transfer enhancement in a double pipe heat exchanger with a twisted inner pipe. *Heat Transfer, 50*(8), 8121–8133. https://doi.org/10.1002/htj.22269.

ANSYS Fluent User's Guide (2011). ANSYS Inc., South pointe 275 Technology Drive Canonsburg.

Bejan, A., Alalaimi, M., Lorente, S., Sabau, A., & Klett, J. (2016, August). Counterflow heat exchanger with core and plenums at both ends. *International Journal of Heat and Mass Transfer, 99*, 622–629. https://doi.org/10.1016/j.ijheatmasstransfer.2016.03.117.

Bell, K. J., Mueller, A. C., & Wolverine, O. O. T. S. C. (1984, January 1). Engineering Data Book Two.

Bergles, A. E. (1998). Techniques to augment heat transfer. In W. M. Bohsenow, J. P. Hartnett & Y.I. Cho (Eds.), *Hand book of Heat Transfer* (3rd ed., Ch. 11). McGraw-Hill.

Bergles, A.E. & Morton, H.L. (1965). Survey and Evaluation of Techniques to Augment Convective Heat Transfer. In MIT Engineering Projects Laboratory (No. 5382–34).

Bright Hub Engineering. (n.d.). http://brighthubengineering.com/.

Cavda, N. K. (2014, December 25). Effect of Nano fluid On Heat Transfer Characteristics of Double Pipe Heat Exchanger: Part-I: Effect of Aluminum Oxide Nano fluid. *International Journal of Research in Engineering and Technology, 03*(12), 42–52. https://doi.org/10.15623/ijret.2014.0312006.

Chen, H. T., & Hsu, W. L. (2007, May). Estimation of heat transfer coefficient on the fin of annular-finned tube heat exchangers in natural convection for various fin spacings. *International Journal of Heat and Mass Transfer, 50*(9–10), 1750–1761. https://doi.org/10.1016/j.ijheatmasstransfer.2006.10.021.

Chen, H. T., & Hsu, W. L. (2008, April). Estimation of heat-transfer characteristics on a vertical annular circular fin of finned-tube heat exchangers in forced convection. *International Journal of Heat and Mass Transfer, 51*(7–8), 1920–1932. https://doi.org/10.1016/j.ijheatmasstransfer.2007.06.035.

Chintan, P., Pragna, P., Jatin, P. & Umang, P. (2012). A Review of heat transfer enhancement using twisted tape. *International Journal of advanced engineering Research and Studies*, *2*(1), 162-164.

Conté, I., & Peng, X. (2009, June). Numerical and experimental investigations of heat transfer performance of rectangular coil heat exchangers. *Applied Thermal Engineering, 29*(8–9), 1799–1808. https://doi.org/10.1016/j.applthermaleng.2008.08.013.

Córcoles, J., Moya-Rico, J., Molina, A., & Almendros-Ibáñez, J. (2020, December). Numerical and experimental study of the heat transfer process in a double pipe heat exchanger with inner corrugated tubes. *International Journal of Thermal Sciences, 158*, 106526. https://doi.org/10.1016/j.ijthermalsci.2020.106526.

Dewan, A., Mahanta, P., Raju, K. S., & Kumar, P. S. (2004, November 1). Review of passive heat transfer augmentation techniques. Proceedings of the Institution of Mechanical Engineers. *Journal of Power and Energy, 218*(7), 509–527. https://doi.org/10.1243/0957650042456953

Ding, Z.W., Cheah, S. C., Nawaf, H. S. (2009). Parametric Study of Heat Transfer Enhancement Using Nanofluids. *Proceeding of International Conference on Energy and Environment*, *Malacca, Malaysia,* 348-352.

Duangthongsuk, W., & Wongwises, S. (2008, December). Effect of thermophysical properties models on the predicting of the convective heat transfer coefficient for low concentration nanofluid. *International Communications in Heat and Mass Transfer,* *35*(10), 1320–1326. https://doi.org/10.1016/j.icheatmasstransfer.2008.07.015.

Duangthongsuk, W., & Wongwises, S. (2009, March). Heat transfer enhancement and pressure drop characteristics of TiO_2–water nanofluid in a double-tube counter flow heat exchanger. *International Journal of Heat and Mass Transfer, 52*(7–8), 2059–2067. https://doi.org/10.1016/j.ijheatmasstransfer.2008.10.023.

Eiamsa-ard, S., Thianpong, C., & Promvonge, P. (2006, December). Experimental investigation of heat transfer and flow friction in a circular tube fitted with regularly spaced twisted tape elements. *International Communications in Heat and Mass Transfer, 33*(10), 1225–1233. https://doi.org/10.1016/j.icheatmasstransfer.2006.08.002.

Eiamsa-ard, S., Wongcharee, K., & Sripattanapipat, S. (2009, November). 3-D Numerical simulation of swirling flow and convective heat transfer in a circular tube induced by means of loose-fit twisted tapes. *International Communications in Heat and Mass Transfer, 36*(9), 947–955. https://doi.org/10.1016/j.icheatmasstransfer.2009.06.014.

Emily, P. (2008). *Force convection in Nano fluid over a flat plate* [MSc thesis, Missouri university].

Esmaeilzadeh, E., Almohammadi, H., Nasiri Vatan, S., & Omrani, A. (2013, January). Experimental investigation of hydrodynamics and heat transfer characteristics of γ-Al_2O_3/water under laminar flow inside a horizontal tube. *International Journal of Thermal Sciences, 63*, 31–37. https://doi.org/10.1016/j.ijthermalsci.2012.07.001.

Farajollahi, B., Etemad, S., & Hojjat, M. (2010, January). Heat transfer of nanofluids in a shell and tube heat exchanger. *International Journal of Heat and Mass Transfer, 53*(1–3), 12–17. https://doi.org/10.1016/j.ijheatmasstransfer.2009.10.019.

Firas, A. A. (2014). *Augmentation of Heat Transfer by Using Nanotechnology* [M.Sc. thesis, Al–Mustansiriya University, Mechanical Engineering Department].

Ghorbani, N., Taherian, H., Gorji, M., & Mirgolbabaei, H. (2010, October). Experimental study of mixed convection heat transfer in vertical helically coiled tube heat exchangers. *Experimental Thermal and Fluid Science, 34*(7), 900–905. https://doi.org/10.1016/j.expthermflusci.2010.02.004.

Ghorbani, N., Taherian, H., Gorji, M., & Mirgolbabaei, H. (2010, August). An experimental study of thermal performance of shell-and-coil heat exchangers. *International Communications in Heat and Mass Transfer, 37*(7), 775–781. https://doi.org/10.1016/j.icheatmasstransfer.2010.02.001.

Gomaa, A., Halim, M., & Elsaid, A. M. (2016, April). Experimental and numerical investigations of a triple concentric-tube heat exchanger. *Applied Thermal Engineering,* *99*, 1303–1315. https://doi.org/10.1016/j.applthermaleng.2015.12.053.

Gorman, J. M., Krautbauer, K. R., & Sparrow, E. M. (2016, August). Thermal and fluid flow first-principles numerical design of an enhanced double pipe heat exchanger. *Applied Thermal Engineering, 107*, 194–206. https://doi.org/10.1016/j.applthermaleng.2016.06.134.

Gupta, J. P. (1986, January 1). *Fundamentals of Heat Exchanger and Pressure Vessel Technology*. Taylor & Francis Group.

Halici, F., & Taymaz, I. (2005, November 11). Experimental study of the airside performance of tube row spacing in finned tube heat exchangers. *Heat and Mass Transfer, 42*(9), 817–822. https://doi.org/10.1007/s00231-005-0042-1.

Han, X., & Wang, Y. (2018, December). Experimental investigation of the thermal performance of a novel concentric tube heat pipe heat exchanger. *International Journal of Heat and Mass Transfer, 127*, 1338–1342. https://doi.org/10.1016/j.ijheatmasstransfer.2018.07.116.

Home - API Heat Transfer. (2023, October 24). API Heat Transfer. http://apiheattransfer.com/.

Incropera, F. P., David P. D., Theodore, L. B. & Adrienne's, S. L. (2007). *Introduction to Heat Transfer*. John Wiley & Sons Inc.

Iqbal, Z., Syed, K., & Ishaq, M. (2013, March). Optimal fin shape in finned double pipe with fully developed laminar flow. *Applied Thermal Engineering, 51*(1–2), 1202–1223. https://doi.org/10.1016/j.applthermaleng.2012.10.036.

JACOBI, A. M. & SHAH, R. K. (1998, January). Air-Side Flow and Heat Transfer in Compact Heat Exchangers: A Discussion of Enhancement Mechanisms. *Heat Transfer Engineering, 19*(4), 29–41. https://doi.org/10.1080/01457639808939934

Kakac, S., Liu, H. (2002). *Heat exchangers selection, rating and thermal design* (2nd Ed.). FL: CRC press. Florida.

Kays, W. M. & London, A. L. (1998). *Compact heat exchangers* (Repr. 3 ed. 1998 with corrections). Krieger Pub.

Kevin G.W. (2010). *Research in heat transfer with Nano fluids* [MSc thesis].

Kharat, R., Bhardwaj, N., & Jha, R. (2009, December). Development of heat transfer coefficient correlation for concentric helical coil heat exchanger. *International Journal of Thermal Sciences, 48*(12), 2300–2308. https://doi.org/10.1016/j.ijthermalsci.2009.04.008.

Kim, Y., & Kim, Y. (2005, September). Heat transfer characteristics of flat plate finned-tube heat exchangers with large fin pitch. *International Journal of Refrigeration, 28*(6), 851–858. https://doi.org/10.1016/j.ijrefrig.2005.01.013.

Lai, W.Y., Duculescu B. & Phelan, A. (2006). *Proceedings of ASME International Mechanical Engineering Congress and Exposition*. Chicago, USA.

Lars, D. (2015). *An Introduction to Turbulence Models, Department of Thermo and Fluid Dynamics*, Chalmers University of Technology, Sweden.

Lee, D. H., Jung, J. M., Ha, J. H., & Cho, Y. I. (2012, February). Improvement of heat transfer with perforated circular holes in finned tubes of air-cooled heat exchanger. *International Communications in Heat and Mass Transfer, 39*(2), 161–166. https://doi.org/10.1016/j.icheatmasstransfer.2011.11.009.

Lee, S., Choi, S. U. S., Li, S., & Eastman, J. A. (1999, May 1). Measuring Thermal Conductivity of Fluids Containing Oxide Nanoparticles. *Journal of Heat Transfer, 121*(2), 280–289. https://doi.org/10.1115/1.2825978.

Lishan, Y. (2002). *Computational Modeling of Laminar Swirl Flows and Heat Transfer in Circular Tubes with Twisted-Tape Inserts* [MSc thesis, University of Cincinnati, Department of Mechanical, Industrial and Nuclear Engineering, College of Engineering].

Lo, C. H., Tsung, T. T., Chen, L. C., Su, C. H., & Lin, H. M. (2005, June). Fabrication of copper oxide nanofluid using submerged arc nanoparticle synthesis system

(SANSS). *Journal of Nanoparticle Research, 7*(2–3), 313–320. https://doi.org/10.1007/s11051-004-7770-x.

Mathanraj, V., Leela Krishna, V., Venkanna Babu, J. L., & Arul Kumar, S. (2018, September 20). Experimental investigation on heat transfer in double pipe heat exchanger employing triangular fins. *IOP Conference Series: Materials Science and Engineering, 402*, 012137. https://doi.org/10.1088/1757-899x/402/1/012137.

Mirgolbabaei, H., Taherian, H., Domairry, G., & Ghorbani, N. (2011, June). Numerical estimation of mixed convection heat transfer in vertical helically coiled tube heat exchangers. *International Journal for Numerical Methods in Fluids, 66*(7), 805–819. https://doi.org/10.1002/fld.2284.

Mon, M. S. (2003). *Numerical Investigation of Air-Side Heat Transfer and Pressure Drop in Circular Finned-Tube Heat Exchangers* [PhD. dissertation, Technische Universitat Bergakademie Freiberg]. Freiberg, Germany.

Mon, M. S., & Gross, U. (2004, April). Numerical study of fin-spacing effects in annular-finned tube heat exchangers. *International Journal of Heat and Mass Transfer, 47*(8–9), 1953–1964. https://doi.org/10.1016/j.ijheatmasstransfer.2003.09.034.

Nagarani, N. & Mayilsamy, K. (2010). Experimental Heat Transfer Analysis on Annular Circular and Elliptical Fins. *International Journal of Engineering Science and Technology, 2*(7), 2839-2845.

Naphon, P., & Wongwises, S. (2002, August). AN EXPERIMENTAL STUDY ON THE IN-TUBE CONVECTIVE HEAT TRANSFER COEFFICIENTS IN A SPIRAL COIL HEAT EXCHANGER. *International Communications in Heat and Mass Transfer, 29*(6), 797–809. https://doi.org/10.1016/s0735-1933(02)00370-6.

Piroozfam, N., Hosseinpour Shafaghi, A., & Razavi, S. (2018, November). Numerical investigation of three methods for improving heat transfer in counter-flow heat exchangers. *International Journal of Thermal Sciences, 133*, 230–239. https://doi.org/10.1016/j.ijthermalsci.2018.07.033.

Prabhanjan, D., Raghavan, G., & Rennie, T. (2002, February). Comparison of heat transfer rates between a straight tube heat exchanger and a helically coiled heat exchanger. *International Communications in Heat and Mass Transfer, 29*(2), 185–191. https://doi.org/10.1016/s0735-1933(02)00309-3.

Qian, S., Yu, J., & Yan, G. (2017, March). A review of regenerative heat exchange methods for various cooling technologies. *Renewable and Sustainable Energy Reviews*, *69*, 535–550. https://doi.org/10.1016/j.rser.2016.11.180.

Rahimi, M., Shabanian, S. R., & Alsairafi, A. A. (2009, March). Experimental and CFD studies on heat transfer and friction factor characteristics of a tube equipped with modified twisted tape inserts. *Chemical Engineering and Processing: Process Intensification, 48*(3), 762–770. https://doi.org/10.1016/j.cep.2008.09.007.

Rahmah, A. M. (2011). *Experimental Study of an Integral Finned–Tube Heat Exchanger* [MSc thesis, University of Technology–Mechanical Engineering Department].

Rebay, S. (1993, May). Efficient Unstructured Mesh Generation by Means of Delaunay Triangulation and Bowyer-Watson Algorithm. *Journal of Computational Physics, 106*(1), 125–138. https://doi.org/10.1006/jcph.1993.1097.

Rostamzadeh, A., Jafarpur, K., Goshtasbirad, E. & Doroodmand, M. M. (2014). Experimental Investigation of Mixed Convection Heat Transfer in Vertical Tubes by Nanofluid: Effects of Reynolds Number and Fluid Temperature, *International Journal of Engineering, 27* (8), 1251-1258.

Sadik, K. & Hongtan, L. (2002). *Heat Exchangers Selection, Rating and Thermal Design* [2nd Ed., Department of Mechanical Engineering, University of Miami]. Coral Gables, Florida.

Saeid, N. H. (2011, December 20). Investigation of thermal performance of air to water heat exchanger using nano-fluids. *IIUM Engineering Journal, 12*(3). https://doi.org/10.31436/iiumej.v12i3.107.

Sahiti, N., Durst, F., & Dewan, A. (2005, November). Heat transfer enhancement by pin elements. *International Journal of Heat and Mass Transfer, 48*(23–24), 4738–4747. https://doi.org/10.1016/j.ijheatmasstransfer.2005.07.001.

Said, Z., Sajid, M., Alim, M., Saidur, R., & Rahim, N. (2013, November). Experimental investigation of the thermophysical properties of AL_2O_3-nanofluid and its effect on a flat plate solar collector. *International Communications in Heat and Mass Transfer, 48*, 99–107. https://doi.org/10.1016/j.icheatmasstransfer.2013.09.005.

Salimpour, M. (2008, November). Heat transfer characteristics of a temperature-dependent-property fluid in shell and coiled tube heat exchangers. *International Communications in Heat and Mass Transfer, 35*(9), 1190–1195. https://doi.org/10.1016/j.icheatmasstransfer.2008.07.002.

Salimpour, M. (2009, January). Heat transfer coefficients of shell and coiled tube heat exchangers. *Experimental Thermal and Fluid Science, 33*(2), 203–207. https://doi.org/10.1016/j.expthermflusci.2008.07.015.

Salman, S. D., Kadhum, A. A. H., Takriff, M. S., & Mohamad, A. B. (2013). CFD Analysis of Heat Transfer and Friction Factor Characteristics in a Circular Tube Fitted with Quadrant-Cut Twisted Tape Inserts. *Mathematical Problems in Engineering, 2013*, 1–8. https://doi.org/10.1155/2013/273764.

Senthilraja, S. & Vijayakumar, KCK. (2013). Analysis of Heat Transfer Coefficient of CuO/Water Nanofluid using Double Pipe Heat Exchanger. *International Journal of Engineering Research and Technology, 6* (5), 675-680.

Shah, R. K. (1975). *Thermal Entry Length Solutions for the Circular Tubes and Parallel Plates*. Indian Institute of Technology, Bombay, 11-75.

Shah, R. K., & Sekulic, D. P. (2003, August 11). *Fundamentals of Heat Exchanger Design*. John Wiley & Sons.

Shankar, R. S. (2012). *Heat transfer in Flow Through Conduits*. Department of Chemical and Biomolecular Engineering Clarkson University.

Shuai, S., Chang. Q. Y. (2011). Numerical Study of Heat Transfer and Pressure Drop of Integral Pin–Fin Tubes. *978*(1), 4244- 6255-1/11.

Srisawad, K., & Wongwises, S. (2008, September 27). Heat transfer characteristics of a new helically coiled crimped spiral finned tube heat exchanger. *Heat and Mass Transfer, 45*(4), 381–391. https://doi.org/10.1007/s00231-008-0441-1.

Sudarmadji, S., Soeparman, S., Wahyudi, S., & Hamidy, N. (2014). Effects of cooling process of Al_2O_3-water nanofluid on convective heat transfer. *FME Transaction, 42*(2), 155–160. https://doi.org/10.5937/fmet1402155s.

Tijing, L. D., Pak, B. C., Baek, B. J., & Lee, D. H. (2006, July). A study on heat transfer enhancement using straight and twisted internal fin inserts. *International Communications in Heat and Mass Transfer, 33*(6), 719–726. https://doi.org/10.1016/j.icheatmasstransfer.2006.02.006.

Verma, T. N., Nashine, P., Singh, D. V., Singh, T. S., & Panwar, D. (2017, June). ANN: Prediction of an experimental heat transfer analysis of concentric tube heat exchanger with corrugated inner tubes. *Applied Thermal Engineering, 120*, 219–227. https://doi.org/10.1016/j.applthermaleng.2017.03.126.

Wang C. C., Chi K. Y., Chang Y. J. & Chang Y. P. (1998). *A Comparison Study of Compact Plate Fin–and–Tube Heat Exchangers*. ASHRAE Transactions.

Warren, D. S. (1968). *Investigation of Heat Transfer Augmentation through Use of Internally Finned Tubes* [MSc thesis, Massachusetts Institute of Technology, Mechanical Engineering Department].

Wasp, E. J., Kenny, J. P. & Grndhi, R. L. (1977). Solid–Liquid Flow Slurry Pipeline Transportation. Series on Bulk Materials Handling, *Trans Techno Publications*, *1*, 4-42.

Webb, R.L. (1987). Enhancement of Single-Phase Convective Heat Transfer. In S. Kakac, R. K. Shah, & W. Aung (Eds.), *Handbook of single-Phase Convective Heat Transfer*. John Wiley and Sons, New York,

Wen, D., & Ding, Y. (2004, November). Experimental investigation into convective heat transfer of nanofluids at the entrance region under laminar flow conditions. *International Journal of Heat and Mass Transfer, 47*(24), 5181–5188. https://doi.org/10.1016/j.ijheatmasstransfer.2004.07.012.

Yu, W., France, D. M., Routbort, J. L., & Choi, S. U. S. (2008, May). Review and Comparison of Nanofluid Thermal Conductivity and Heat Transfer Enhancements. *Heat Transfer Engineering, 29*(5), 432–460. https://doi.org/10.1080/01457630701850851.

Zeinali Heris, S., Nasr Esfahany, M. & Etemad S. Gh. (2006). *Heat Transfer Enhancement of Nanofluid Laminar Flow* [Conference presentation]. 18th Annual (International) Mechanical Engineering Conference.

CURRICULUM VITAE

Student Information	
Name/Surname:	Mohammed Flayyih HASAN
Nationality:	IRAQ
Orcid No:	0000-0002-5112-8261

School Information	
Undergraduate Study	
University	ANBAR UNIVERSITY
Faculty	FACULTY OF ENGINEERING
Department	MECHANICAL ENGINEERING
Graduation Year	2001-2002
Graduate Study	
University	KIRŞEHİR AHİ EVRAN UNIVERSİTY
Institute	INSTITUTE OF NATURAL AND APPLIED SCIENCES
Department	MECHANİCAL ENGİNEERİNG
Graduation Year	2023

Articles and Papers Produced from the Thesis
HASAN, M. F., DANIŞMAZ, M., & WAHEED, F. (2022, March 31). Modern Nanotechnology Application for Generation Highly Efficient Electricity in Save Mode and Much Less Polluting. *International Journal of Computational and Experimental Science and Engineering, 8*(1), 1–4. https://doi.org/10.22399/ijcesen.1035440.   Hasan, M. F., Danışmaz, M., & Majel, B. M. (2023, March). Thermal performance investigation of double pipe heat exchanger embedded with extended surfaces using nanofluid technique as enhancement. *Case Studies in Thermal Engineering, 43*, 102774. https://doi.org/10.1016/j.csite.2023.102774.